Spatial distribution and size evolution of particles in Asian outflow: Significance of primary and secondary aerosols during ACE-Asia and TRACE-P

Cameron S. McNaughton,[1] Antony D. Clarke,[1] Steven G. Howell,[1] Kenneth G. Moore II,[1] Vera Brekhovskikh,[1] Rodney J. Weber,[2] Douglas A. Orsini,[2] David S. Covert,[3] Gintautas Buzorius,[4,5] Fred J. Brechtel,[4,6] Gregory R. Carmichael,[7] Youhua Tang,[7] Fred L. Eisele,[2,8] R. Lee Mauldin,[8] Alan R. Bandy,[9] Donald C. Thornton,[9] and Byron Blomquist[1,9]

Received 23 February 2003; revised 2 March 2004; accepted 13 May 2004; published 14 September 2004.

[1] Quasi-Lagrangian aircraft measurements above the Yellow Sea, East China Sea, and Sea of Japan revealed synoptic-scale secondary aerosol formation and condensational growth during the Asian Pacific Regional Aerosol Characterization Experiment (ACE-Asia) and Transport and Chemical Evolution over the Pacific (TRACE-P) experiment. This occurred in the presence of pollution and mineral dust aerosol surface areas as high as 1200 μm^2 cm^{-3}. Concentrations of sulfuric acid generally appeared insufficient for binary nucleation, but observations, models, and theory are consistent with a ternary nucleation mechanism involving H_2SO_4-H_2O-NH_3. Growth rates of $\sim$2 nm h^{-1} can be explained by the condensation of sulfuric acid at a rate of $2 \pm 1 \times 10^6$ molecules cm^{-3} s^{-1}. Aerosol volatility suggested increasing neutralization of the aerosol during growth. Size distribution measurements suggest that weak (mean condensation nuclei (CN) 3–13 nm $\approx$ 500 cm^{-3}) new particle production was a common occurrence in the region. However, new particle production was enhanced by $\sim$1 order of magnitude (mean CN 3–13 nm $\approx$ 5000 cm^{-3}) in postfrontal air masses associated with offshore flow during cloud-free conditions. Fog and clouds appear to be regionally important in modulating nucleation events through scavenging of secondary aerosol and through depletion of gas-phase precursors through enhanced heterogeneous chemistry. Our results indicate that only 10–30% of the total aerosol population consists of aged secondary aerosols after $\sim$2 days of transport from source regions. In spite of their high production during nucleation events, secondary aerosols advected out over the Pacific Ocean will have a small impact upon indirect forcing and a negligible impact upon direct forcing compared to primary aerosol emissions and the species that condense upon them. *INDEX TERMS:* 0305 Atmospheric Composition and Structure: Aerosols and particles (0345, 4801); 4801 Oceanography: Biological and Chemical: Aerosols (0305); 0345 Atmospheric Composition and Structure: Pollution—urban and regional (0305); 0368 Atmospheric Composition and Structure: Troposphere—constituent transport and chemistry; 9320 Information Related to Geographic Region: Asia; *KEYWORDS:* ACE-Asia, TRACE-P, aerosol size distribution, nucleation, primary and secondary aerosols, condensation and coagulation

Citation: McNaughton, C. S., et al. (2004), Spatial distribution and size evolution of particles in Asian outflow: Significance of primary and secondary aerosols during ACE-Asia and TRACE-P, *J. Geophys. Res.*, *109*, D19S06, doi:10.1029/2003JD003528.

1. Introduction

[2] The *Intergovernmental Panel on Climate Change* [2001] has recently indicated that our understanding of the origin and evolution of aerosols as well as their impact

[1]School of Ocean and Earth Science and Technology, University of Hawaii, Honolulu, Hawaii, USA.
[2]School of Earth and Atmospheric Sciences, Georgia Institute of Technology, Atlanta, Georgia, USA.
[3]Department of Atmospheric Sciences, University of Washington, Seattle, Washington, USA.
[4]Atmospheric Sciences Division, Brookhaven National Laboratory, Upton, New York, USA.
[5]Now at Center for Interdisciplinary Remotely-Piloted Aircraft Studies, Naval Postgraduate School, Marina, California, USA.
[6]Now at Brechtel Manufacturing, Inc., Hayward, California, USA.
[7]Department of Chemical and Biochemical Engineering, University of Iowa, Iowa City, Iowa, USA.
[8]Atmospheric Chemistry Division, National Center for Atmospheric Research, Boulder, Colorado, USA.
[9]Department of Chemistry, Drexel University, Philadelphia, Pennsylvania, USA.

0148-0227/04/2003JD003528$09.00

on global climate is inadequate. Natural and anthropogenic aerosols from primary emissions and those formed in situ (secondary aerosols) have the ability to directly affect the Earth's radiative balance by scattering and/or absorbing incoming solar radiation. Additionally, aerosols have the potential to affect the number and size of cloud condensation nuclei (CCN) altering cloud albedo in what is referred to as the aerosol indirect effect [*Albrecht*, 1989; *Twomey*, 1974]. Secondary aerosols are of particular interest because their significance, compared to primary aerosols, is related to whether their growth and removal rates result in conditions where they contribute "new" number to the background atmosphere. Interest in issues related to secondary aerosol formation has stimulated a variety of experiments designed to investigate these processes [*Kulmala et al.*, 2004].

[3] With regard to the nucleation mechanism, *Kulmala et al.* [2002] showed that new particles were forming via a ternary nucleation mechanism involving H_2SO_4, H_2O and NH_3 during the Particle Formation and Fate in the Coastal Environment (PARFORCE) experiment. *O'Dowd et al.* [2002a, 2002b] demonstrated that H_2SO_4 concentrations were insufficient to produce the observed particle growth during PARFORCE and found that photo-oxidation of the organic compound CH_2I_2 (from exposed tidal flats) contributed the mass necessary to explain the growth rate of the nucleation mode aerosol. At a clean continental site on the eastern slope of the Rocky Mountains in Colorado, *Weber et al.* [1997] found concentrations of H_2SO_4 and H_2O during a nucleation event that were well below those required for binary nucleation. In addition, the observed growth rates were approximately 5–10 times higher than the rate predicted from sulfuric acid and water alone. *Leaitch et al.* [1999] could not distinguish whether H_2SO_4 or forest derived organics initiated a nucleation event at a clean continental site in eastern Canada. They did show that subsequent growth of the aerosol could be attributed to organic oxidation products. More recently, *Janson et al.* [2001] observed nucleation over a forest ecosystem at a clean continental site in Finland. They found monoterpene oxidation products were not nucleation precursors but that low-vapor-pressure organics were needed to explain the observed growth rates because of insufficient concentrations of H_2SO_4 and NH_3.

[4] Regardless of the microphysical nature of the newly formed secondary aerosols, *Raes et al.* [2000] suggest that too often we have not examined these secondary aerosols with regard to large-scale atmospheric circulation. Atmospheric processes involving temperature and humidity changes within a single air parcel (atmospheric waves, turbulence, large convective eddies) or mixing of two air parcels with different relative humidity and temperature (gradients and/or entrainment) can enhance binary nucleation for the H_2SO_4 and H_2O system [*Easter and Peters*, 1994; *Kerminen and Wexler*, 1994a; *Nilsson and Kulmala*, 1998]. These same phenomena should enhance any ternary nucleation mechanism involving H_2SO_4, H_2O and NH_3 although the dependence on relative humidity is less than that of the binary system [*Kulmala et al.*, 2002; *Napari et al.*, 2002b]. Large-scale new particle production associated with a particular type of air mass was reported during the European Biogenic Aerosol Formation in the Boreal Forest (BIOFOR) experiment where synoptic-scale new particle formation was observed in the continental boundary layer [*Kulmala et al.*, 2001a]. The BIOFOR study showed that the onset of turbulence and development of the continental boundary layer (CBL) was related to the burst of particle formation while the forest canopy and the free troposphere could be ruled out as the nucleation region [*Buzorius et al.*, 2001; *Nilsson et al.*, 2001].

[5] Airborne measurements of the transport of natural and anthropogenic aerosols throughout the Pacific has been documented [*Clarke et al.*, 2001; *Clarke and Kapustin*, 2002; *Moore et al.*, 2003]. The low aerosol surface areas common in these regions reduces coagulation and can lead to long lifetimes for these particles. However, in polluted regions with high aerosol surface area many of these particles are expected to coagulate with the primary aerosol within 1–2 days [*Raes et al.*, 2000]. These issues were recently investigated as part of two major experiments near Asia. NASA conducted the Transport and Chemical Evolution over the Pacific (TRACE-P) experiment from 26 February to 9 April of 2001. The United States' National Science Foundation (NSF) supported the Asian Pacific Regional Aerosol Characterization Experiment (ACE-Asia) as part of the International Global Atmospheric Chemistry Project (IGAC) from 31 March to 4 May 2001. Both experiments were designed as multinational, multiagency experiments involving ship-based, ground-based, aircraft, and satellite data collection together with real-time forecasting by a number of meteorology and atmospheric chemistry transport models (CTMs) [*Huebert et al.*, 2003; *Jacob et al.*, 2003]. Since the large-scale industrialization of east Asia observations of secondary aerosol formation and growth in the region are underrepresented in the current literature [*Kulmala et al.*, 2004]. Here we examine various cases of recent nucleation evident on specific flights during these two experiments and their implications for understanding aerosol formation and growth over the coastal waters near Asia.

2. Instrumentation Aboard the NASA P3-B and the NCAR C-130

[6] TRACE-P and ACE-Asia had different objectives and participants and therefore different instrumentation. This study focuses on gas and aerosol phase measurements common to the NASA P3-B aircraft during TRACE-P, the NSF/NCAR C-130 aircraft during ACE-Asia and supporting measurements made aboard the R/V *Ron Brown* and at the Gosan surface site during ACE-Asia.

[7] During TRACE-P a modified TSI ultrafine condensation particle counter (model 3025A) equipped with pulse height analysis (PHA-UCN) was operated by the Georgia Institute of Technology aboard the NASA P3-B aircraft. This instrument measures the 1 min average concentration of both 3–4 nm and 3–8 nm particles [*Marti et al.*, 1996; *Saros et al.*, 1996; *Weber et al.*, 1998b]. Soluble inorganic ions (Na^+, K^+, NH_4^+, Ca^{2+}, Mg^{2+}, Cl^-, NO_3^-, SO_4^{2-}) associated with fine particles (diameters less than 1.3 μm) were measured using ion chromatography in the Georgia Institute of Technology particle-into-liquid sampling (PILS) system aboard both the NASA P3-B and the NCAR C-130 [*Orsini et al.*, 2003; *Weber et al.*, 2001b]. Gas-phase SO_2 was

measured on both aircraft by Drexel University using Atmospheric Pressure Ionization Mass Spectrometry (APIMS) with isotopically labeled internal standards [*Thornton et al.*, 2002]. Concentrations of H_2SO_4, OH and MSA were measured exclusively aboard the NASA P3-B by the team from the National Center for Atmospheric Research (NCAR) using a selected ion chemical ionization mass spectrometer (SCIMS) [*Eisele and Tanner*, 1993].

[8] Total light scattering was measured aboard the NASA P3-B using a three-wavelength (450, 550, 700 nm) TSI model 3563 nephelometer operated by the University of Hawaii. Two model 3563 nephelometers aboard the NCAR C-130 were used to measure total and submicrometer scattering by installing a 1 μm aerodynamic impactor in the second nephelometer. More information about the operation and corrections made to the nephelometer data is given by *Anderson et al.* [1996] and *Anderson and Ogren* [1998].

[9] The NCAR radial differential mobility analyzer system (NCAR rDMA) measured the size and number of particles between 0.007 and 0.150 μm with a resolution of 54 channels per decade aboard the C-130 aircraft [*Russell et al.*, 1996]. The University of Hawaii operated radial differential mobility analyzers (rDMAs) and laser optical particle counters (OPCs) aboard both the NASA P3-B and the NCAR C-130. The UH DMA systems operate using a 90 s data scan followed by a 30 s down time (no data recorded). The rDMAs effectively size particles between 0.007 and 0.210 μm with a resolution of 32 logarithmically spaced channels per decade and are coupled to a lagged aerosol grab (LAG) chamber which allows up to three DMA scans per sample volume [*Clarke et al.*, 1998]. The OPC (PMS LAS-X with customized electronics) effectively sizes particles between 0.100 and 14 μm with a resolution of 112 logarithmically spaced channels per decade. OPC distributions are obtained every 30 s. Coupled to both the DMA and OPC sampling systems is the University of Hawaii Thermo-Optical Aerosol Discriminator or TOAD. This simple system of heaters and valves allows the sample to be preheated to ambient cabin temperature, 150°C or 300°C. We use the differences between the heated and unheated size distributions in order to infer aerosol compositional data [*Clarke*, 1991]. In the clean marine boundary layer we have shown that the difference between the dry ambient and the 150°C scan represents primarily sulfuric acid [*Clarke et al.*, 1998]. The TOAD volatilizes ammoniated species such as ammonium sulfate and ammonium bisulfate ($(NH_4)_2SO_4$ and NH_4HSO_4) between 150°C and 300°C. We refer to the aerosol volume remaining after 300°C as the "refractory component" which typically consists of black carbon species, fly ash, sea salt and/or mineral dust. The polluted marine environment of the ACE-Asia and TRACE-P study region makes the interpretation of volatile species more uncertain because of our inability to distinguish between sulfate aerosols and nitrates, organic aerosols and other components volatile at temperatures <300°C. However, a strong correlation (R^2 = 0.77) and slope of 1.05 between size-resolved OPC volatile mass and measurements of aerosol soluble ions and organic carbon indicate that this approach is closely related to the aerosol chemistry (S. Howell et al., manuscript in preparation, 2004).

[10] Total particle concentrations were measured aboard the R/V *Ron Brown* using a TSI model 3025 (CN > 3 nm) and a TSI model 3760 CN (CN > 13 nm) counter. Total particle concentrations at ambient cabin temperature and after heating to 300°C (to identify so-called refractory CN or RCN) were measured aboard the P3-B using two TSI model 3010 CN counters with a 50% counting efficiency at 10 nm. Total particle concentrations were measured aboard the C-130 using a TSI model 3025 CN counter (CN > 3 nm) with a 50% counting efficiency at 3 nm. However, we note that under some observed concentrations of sulfuric acid (e.g., volcanic plumes near Japan) some errors in counting efficiency may be inherent in the results because of chemical reactions between sulfuric acid and the n-butyl alcohol used in the CN counters [*Hanson et al.*, 2002]. Two TSI model 3760 CN counters with a 50% counting efficiency at 13 nm were operated aboard the C-130 by the NCAR Research Aviation Facility and the University of Hawaii. A single model 3760 sampled air previously heated to 300°C aboard the C-130 (RCN). Volatile CN (VCN) is defined as the difference between the CN counters operating at ambient cabin temperature and those previously heated to 300°C. All particle concentrations are reported at standard atmospheric temperature and pressure (SATP, P = 101.325 kPa, T = 298.15 K).

3. Parameterization of the Binary and Ternary Nucleation Rate

[11] In our discussion of secondary aerosol formation we will use two parameterizations for predicting whether the observed new particle formation is likely the result of a binary nucleation mechanism involving H_2SO_4 and H_2O or a ternary nucleation mechanism involving H_2SO_4, NH_3 and H_2O. The binary parameterization is that of *Vehkamäki et al.* [2002]

$$C_{\text{binary}} = \exp\left(\begin{array}{l}-279.243 + 11.7344\cdot \text{RH} + \frac{22700.9}{T} - 1088.64\frac{\text{RH}}{T} + 1.14436\cdot T - 0.0302331\cdot \text{RH}\cdot T\ldots \\ -0.00130254\cdot T^2 - 6.38697\cdot \log(\text{RH}) + 854.98\frac{\log(\text{RH})}{T} + 0.00879662\cdot T\cdot \log(\text{RH})\end{array}\right), \quad (1)$$

where RH and T are relative humidity (0–1) and temperature in Kelvin. C_{binary} predicts the threshold concentration (molecules cm^{-3}) of sulfuric acid necessary to achieve a nucleation rate, J, of 1 cm^{-3} s^{-1}. The equation is valid between 230.15 K and 305.15 K and between 0.01 and 100% relative humidity Modeling by *Pirjola et al.* [2000] suggests that binary nucleation only occurs under extreme conditions when free troposphere air containing very low aerosol condensation sinks and high sulfuric acid concentrations (>10^8 molecules cm^{-3}) is entrained into the marine boundary layer. They suggest that instead a ternary nucleation mechanism involving H_2SO_4, H_2O and NH_3 predicts new particle formation under more realistic sulfuric acid (1.2×10^7 molecules cm^{-3}) and ammonia (>5 pptv) concentrations for the unperturbed marine boundary layer (MBL).

[12] To examine whether ternary nucleation is possible under the observed conditions of temperature and relative humidity we use the method of *Napari et al.* [2002c]. The ternary parameterization is valid from 240 to 300 K, from 5 to 95% relative humidity for sulfuric acid concentrations between 10^4 and 10^9 molecules cm^{-3}, for ammonia mixing ratios of 0.1–100 pptv and for nucleation rates between

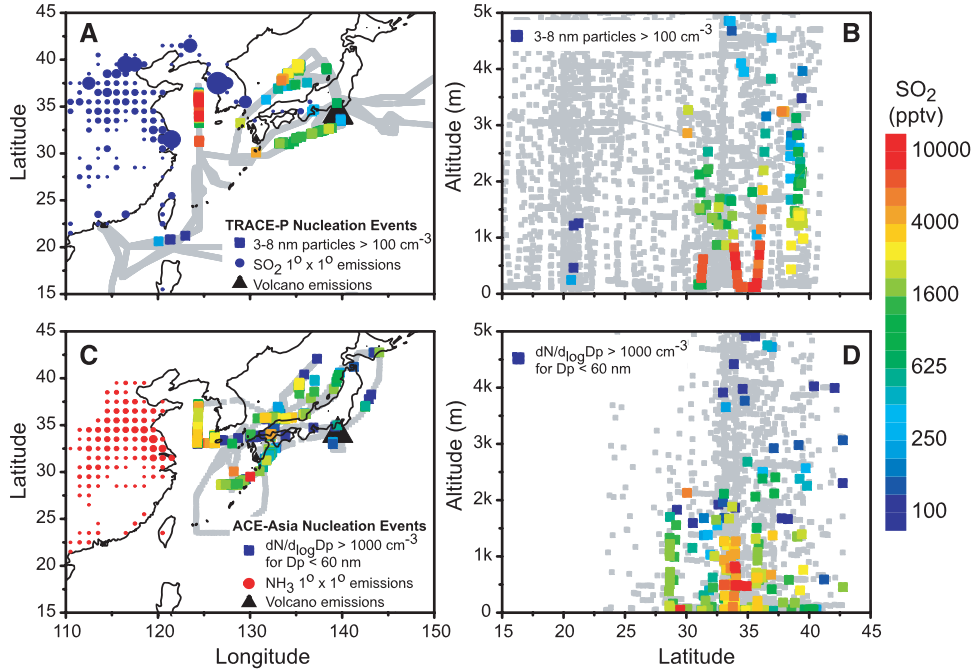

Figure 1. Plan and meridional views of nucleation events (a and b) for TRACE-P from PHA-UCN analysis and (c and d) for ACE-Asia from rDMA analysis. Panels include top two hundred 1° × 1° source regions for SO_2 and NH_3, local volcanic emissions of SO_2, and sample locations where nucleation events were not observed (gray boxes).

10^{-5} and 10^{6} cm^{-3} s^{-1}. Gas-phase ammonia measurements were not made during ACE-Asia or TRACE-P. Therefore, instead of solving for the nucleation rate, J, based on T, RH, concentrations of gas-phase sulfuric acid and ammonia we use the ternary parameterization to predict the concentration of H_2SO_4 required to produce a fixed nucleation rate (J = 10^{5} cm^{-3} s^{-1}) for a fixed concentration of ammonia (10 or 100 pptv).

[13] The ternary parameterization is the first of its kind whereas the binary parameterization is a substantial improvement over more traditional parameterization [*Jaecker-Voirol and Mirabel*, 1989; *Kulmala et al.*, 1998; *Wexler et al.*, 1994; *Wilemski*, 1984]. This is the first comparison of these parameterizations to an observational data set measured aboard a research aircraft.

4. Observations

4.1. Secondary Aerosol Formation on a Synoptic Scale

[14] The top two hundred 1° × 1° SO_2 and NH_3 emission areas in the Asian study region are plotted as scaled circles in Figures 1a and 1c. Each of the plotted SO_2 and NH_3 emission sources exceed 34.5 and 38.2 kt yr^{-1} with the top sources emitting 309 and 113 kt yr^{-1} for SO_2 and NH_3, respectively [*Carmichael et al.*, 2003b; *Streets et al.*, 2003]. The active volcanoes Miyakejima and Sakurajima are also substantial sources of regional SO_2 emitting 8400 and 470 kt SO_2 yr^{-1} and are identified as scaled triangles in Figure 1. Because prevailing winds are westerly during this time of year recently formed nucleation mode (1–10 nm) and/or Aitken mode (10–100 nm) aerosols were typically observed downwind of the urban/industrial regions of Asia with strong sources of SO_2 and NH_3. The highest concentrations of anthropogenic SO_2 recorded by the P3-B and the C-130 aircraft were in the Yellow Sea. Elevated SO_2 concentrations were also identified in the Sea of Japan and south of Japan where Asian outflow was advected toward the Northwest Pacific.

[15] Figure 1 also includes the spatial distribution of cases where nucleation was identified according to two different approaches during TRACE-P and ACE-Asia. The figure also shows cases where little or no evidence for recent nucleation was observed. Figure 1a shows locations for measurements made by the PHA-UCN aboard the P3-B during the TRACE-P campaign. Highlighted boxes show locations where concentration of 3–8 nm particles exceeded 100 particles cm^{-3} and have been shaded by SO_2 concentrations at the time of observation. This approach emphasizes recently nucleated aerosols expected to be less than a few hours old. Figure 1b shows the same data plotted with a meridional view to show the vertical distribution of these nucleation mode particles. Using the rDMA size distributions from ACE-Asia and TRACE-P, we were able to identify recently formed secondary aerosols with mode diameters as large as 40 nm and with tails extending to sizes as large as 60 nm. This approach makes it possible to identify secondary aerosols originating from nucleation events within the previous 24 hours. Figures 1c and 1d show the locations where rDMA size distributions were measured aboard the C-130 during ACE-Asia. Distributions where concentrations of particles with diameter less than 60 nm exceeded 1000 particles cm^{-3} are also shaded by SO_2 concentration at the time of observations.

[16] These two approaches for identifying new particle production reveal a consistent pattern of nucleation events

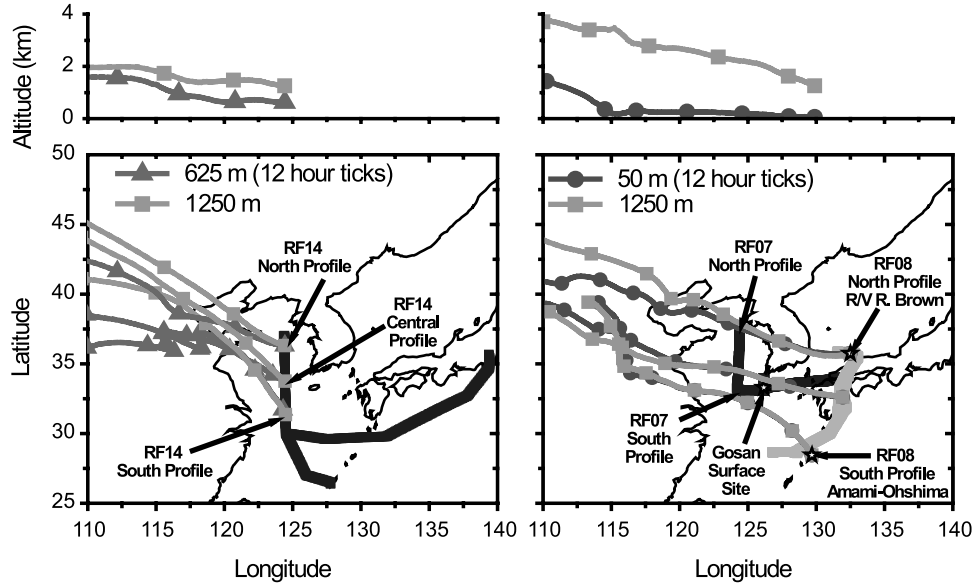

Figure 2. Back trajectories for profiles from (left) TRACE-P flight 14 on 18 March 2001 and (right) ACE-Asia flight 8 on 13 April 2001. The figure also shows locations of profiles during ACE-Asia flight 7 on 12 April and the location of the R/V *Ron Brown*, the Gosan surface site, and the Amami-Ohshima LIDAR installation.

and indicate that the majority of newly formed secondary aerosols were found between 30°N and 38°N and below 2500 m (typical maximum height of the MBL). Most events occurred in air masses associated with SO_2 concentrations in excess of 1 ppbv. Nucleation mode particles appear to be less prevalent in the free troposphere (FT) where SO_2 concentrations rarely exceed 1 ppbv.

4.2. Case Studies

[17] In spite of the strong sources of precursors evident for much of the region the aircraft measurements in Figure 1 indicate that below 2000 m, nucleation events were only observed 33% of the time. This implies that certain conditions favor enhanced nuclei formation, survival, and growth to observable sizes (>3 nm). Specific cases illustrating the importance of atmospheric structure in the formation of secondary aerosols and the influence of primary aerosol surface area upon the concentrations of newly formed particles follow.

4.2.1. On 18 March: TRACE-P Flight 14

[18] On 18 March 2001, meteorological data indicated that surface flow brought air over the industrialized areas of Beijing/Tianjin and into the Yellow Sea at approximately 5–10 m s^{-1}. The outflow was due to a low-pressure system centered east of Honshu Japan and a second northeast of Harbin China (near the border of northeastern China and Siberia). These two low-pressure systems were backed by a high-pressure system located above Wuhan, to the west of Shanghai China. TRACE-P flight 14 (RF14) was designed to intercept this air mass as it was advected from the industrialized regions of northeastern China out over the Yellow Sea. The first column of Figure 2 shows the flight path of the NASA P3-B, location of three profiles, and air mass back trajectories generated by the United States' National Oceanic and Atmospheric Administration (NOAA) Air Resources Laboratory's HYSPLIT model (R. R. Draxler and G. D. Rolph, HYSPLIT (Hybrid Single-Particle Lagrangian Integrated Trajectory) Model access via NOAA ARL READY Website (http://www.arl.noaa.gov/ready/hysplit4.html), NOAA Air Resources Laboratory, 2003).

4.2.2. On 12 and 13 April: ACE-Asia Flights 7 and 8

[19] From 6 to 13 April of 2001 a major dust storm swept through the ACE-Asia study region. The advancing cold front passed the Gosan surface site at Jeju Island South Korea (33.28°N, 126.17°E, alt. 70 m) at ~1600 UTC on 11 April (0100 local time, 12 April). Meteorological conditions show that 5–8 m s^{-1} winds at the 925 mbar level were from the northwest. On 12 April the C-130 conducted field operations in the Yellow Sea including an intercomparison with the Gosan surface site. The air mass encountered on 12 April is characterized as postfrontal and was undergoing synoptic-scale subsidence. The same passing cold front moved over the R/V *Ron Brown*, stationed in the Sea of Japan (35.74°N, 132.50°E), at approximately 0600 UTC, 12 April (1500 local time, 12 April).

[20] A second flight on 13 April involved an intercomparison with the R/V *Ron Brown* in the Sea of Japan followed by an intercomparison with the LIDAR installation at Amami-Ohshima south of Kyushu Japan (28.44°N, 129.70°E). HYSPLIT back trajectories show that the air mass near the surface passed over the industrialized areas of Beijing/Tianjin and into the Yellow and East China Seas. Back trajectories also show the large-scale divergence linked to the subsiding upper air. Because of the synoptic-scale motion of the front and by sampling to the east of the previous days' flight the C-130 completed a quasi-Lagrangian study of essentially the same air mass over a 24 hour period. The flight path for ACE-Asia flights seven (RF07) and eight (RF08), locations of vertical profiles, and

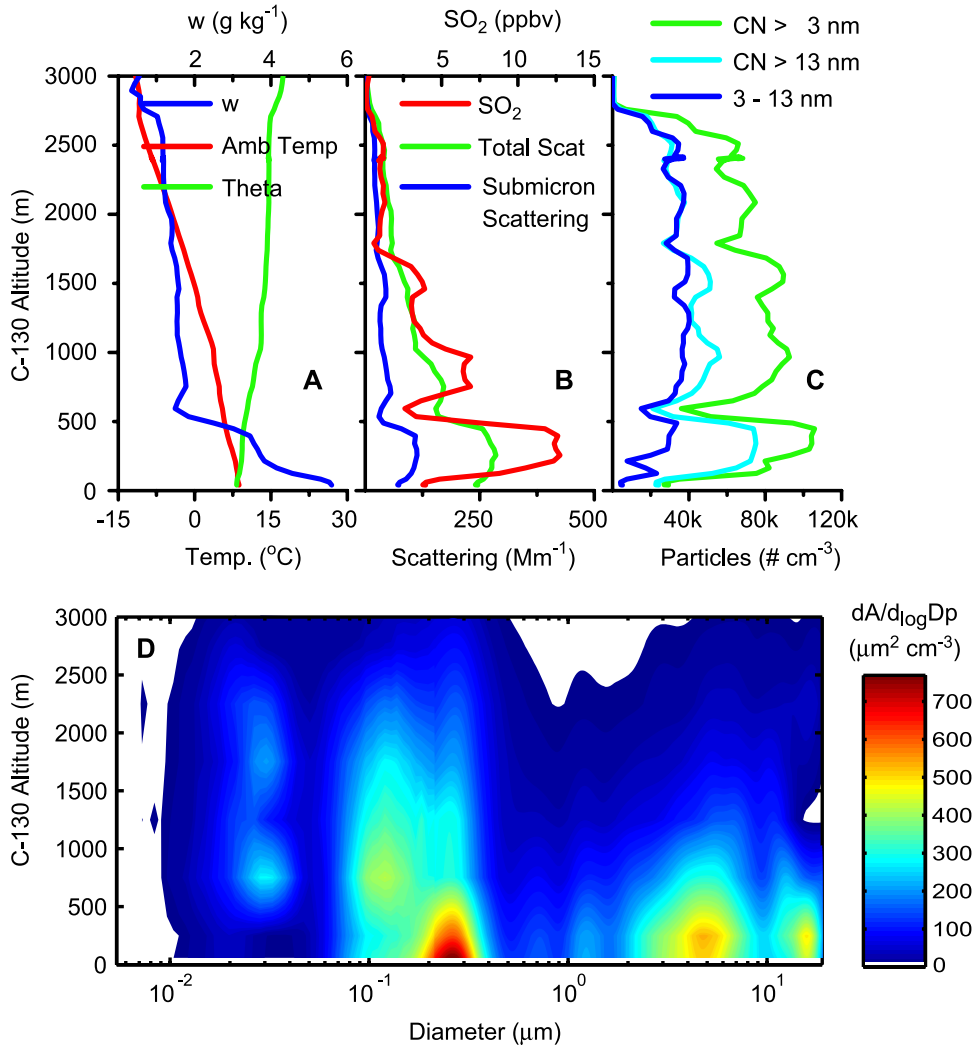

Figure 3. (a) Thermodynamic parameters, (b) SO_2 and light scattering, and (c) particle concentrations during the northern profile of ACE-Asia flight 7. (d) Vertical structure of the aerosol area distributions along 124.4°E during ACE-Asia flight 7.

the locations of the R/V *Ron Brown* and both of the surface sites are shown in the second column of Figure 2.

4.3. Aircraft Profiles and Size Distributions Along 124°E

[21] Variability of thermodynamic properties as well as gas and aerosol parameters were routinely observed on the scale of tens to hundreds of meters during the aircraft vertical profiles over the Yellow Sea (locations shown in Figure 2). Figure 3 illustrates thermodynamic, gas, aerosol and optical properties measured during the northern vertical profile over the Yellow Sea during ACE-Asia flight 7. This profile was typical of other profiles over the Yellow Sea (e.g., northern, central and southern profiles from TRACE-P flight 14) and shows that the boundary layer is divided into the developing marine boundary layer, 200–600 m thick and the pre-existing continental boundary layer (*T* inversion at ~2000–2500 m). Stratification of the layers was evident by near surface temperature inversions and a doubling of water vapor mixing ratio within the shallow layer. Sulfur dioxide, sulfuric acid and nucleation/Aitken mode particles are often depleted near the surface while total and submicrometer scattering are highest within the developing MBL. Aloft SO_2, H_2SO_4, total and submicrometer scattering decrease with height. The 3–13 nm particle concentrations remain high throughout the boundary layer and usually peak at the MBL/CBL interface.

[22] During the central descent profile of TRACE-P flight 14, two rDMA size distributions were measured (Figure 4). The first distribution (Figures 4a and 4c) was recorded at 660 m directly above the developing MBL and the second (Figures 4b and 4d) was recorded at 120 m and therefore within the MBL. The number distribution at 660 m shows a clear nucleation mode aerosol centered at 9 nm but after heating to 150°C all the volume for this mode has been eliminated. This is consistent with the nucleation mode aerosol being composed primarily of sulfuric acid or another compound (e.g., an organic species) volatile at temperatures below 150°C. A second peak, possibly formed earlier, is centered at 40 nm with reduced volatility at 150°C consistent with partial neutralization by ammonia. The accumulation mode aerosol shows a distinct pollution

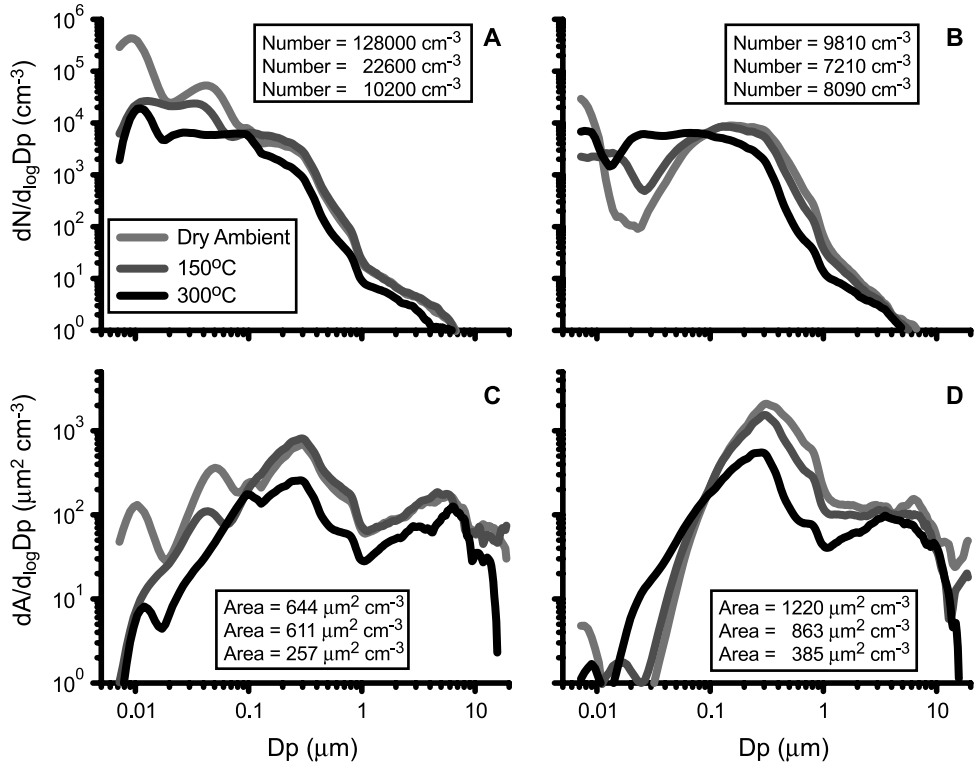

Figure 4. Aerosol number (Figure 4a) and area (Figure 4c) distributions recorded at 660 m above the Yellow Sea along 124.4°E during TRACE-P flight 14. Distribution shows volatile nucleation mode and partially neutralized Aitken/accumulation mode aerosol. Aerosol number (Figure 4b) and area (Figure 4d) distributions recorded at 120 m show fewer nucleation mode particles and a doubling of aerosol surface area. The accumulation mode aerosol is less neutralized, suggesting enhanced production of sulfates in the layer.

signature with a refractory residual related to soot and with low volatility at 150°C consistent with near complete neutralization of the sulfuric acid by ammonia. The molar equivalents ratio ($[NH_4^+]$: $2[SO_4^{2-}] + [NO_3^-]$) as measured by the PILS instrument [*Orsini et al.*, 2003; *Weber et al.*, 2001b] was 1.17, confirming our inferred neutralization of the accumulation mode sulfuric acid to ammonium bisulfate/sulfate based upon aerosol volatility. The SO_2 concentration was 9.6 ppbv, the concentration of sulfuric acid was 6.0×10^7 molecules cm^{-3}. C_{binary} and $C_{ternary}$ were calculated to be 1.3×10^9 molecules cm^{-3} and 8.1×10^6 molecules cm^{-3}. This suggests that the available concentration of sulfuric acid was 22 times too low for binary nucleation and 7 times higher than necessary for ternary nucleation (for $J = 10^5$ cm^{-3} s^{-1} and $[NH_3]$ = 10 pptv). The second distribution, obtained at 120 m, shows nucleation mode particles within the developing MBL are an order of magnitude less numerous than those above the layer while total aerosol surface area has nearly doubled (Figure 4d). SO_2 concentrations have dropped but remain high at 5.1 ppbv (±1.5 ppbv), H_2SO_4 has dropped to 2.2×10^7 molecules cm^{-3} (±0.80) but remains 1.3 times higher than required to satisfy $C_{ternary}$ and 22 times lower than required for C_{binary}. Molar ratios of $[NH_4^+]$:$(2[SO_4^{2-}] + [NO_3^-])$ averaged 0.87 (±0.06) and supports the volatility analysis which shows accumulation mode aerosol has been neutralized to a lesser degree than at 660 m.

[23] Figure 3d shows combined rDMA and OPC area distributions measured during the northern and southern vertical profiles along 124.4°E from ACE-Asia flight 7. The distributions from nearly one month later (12 April versus 18 March 2001) show few nucleation mode particles below 500 m similar to the two distributions shown in Figure 4 during the central profile of TRACE-P flight 14. In the ACE-Asia case the accumulation mode area has a larger mode diameter within the surface layer and is present in conjunction with mineral dust. Recently formed nucleation and Aitken mode particles have their highest concentrations above the MBL and are associated with smaller coarse and accumulation mode surface area. Values for C_{binary} indicate that the most likely site of secondary aerosol formation is within the MBL yet 3–13 nm particle concentrations are lowest within the shallow layer. There is also a second peak in nucleation mode particles aloft where C_{binary} and $C_{ternary}$ indicate that the cold, high-relative-humidity environment favors the formation of nucleation mode particles. At the CBL inversion (~2700), entrainment of low-surface-area free troposphere air during subsidence could also enhance secondary aerosol formation [*Nilsson and Kulmala*, 1998].

[24] Nucleation mode particles within the developing marine boundary layer (<500 m) as measured by CN counters and the rDMAs indicate that gas-to-particle conversion recently occurred. The lower concentrations and smaller diameters of nucleation mode particles below 500 m

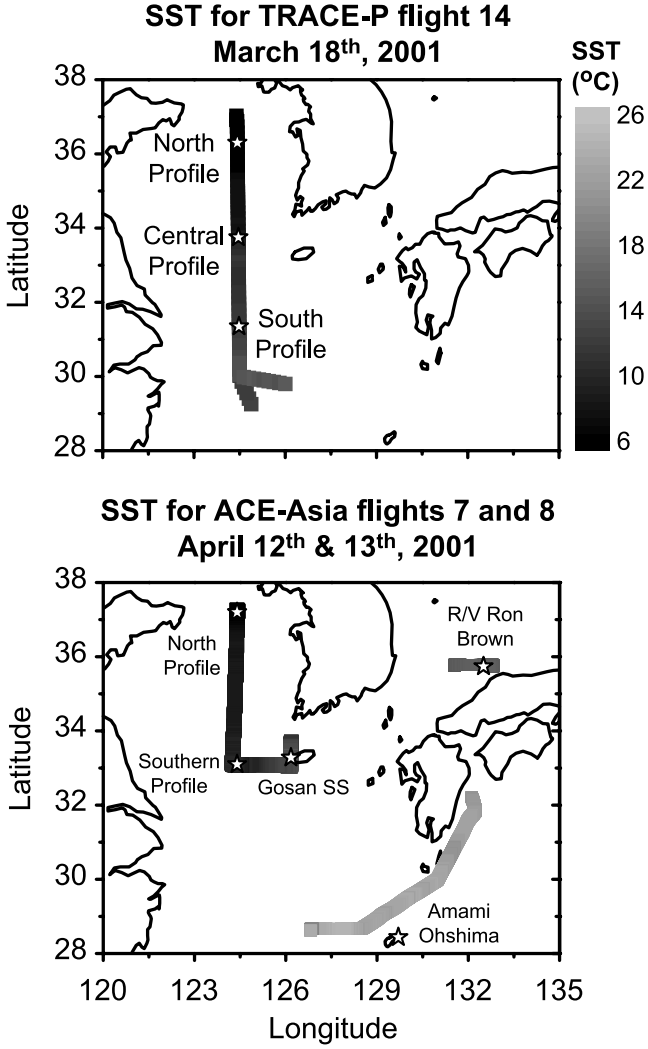

Figure 5. Sea surface temperature measured by infrared sensors aboard the (top) P3-B during TRACE-P flight 14 and (bottom) C-130 during ACE-Asia flights 7 and 8. Waters are cooler near the coast because of spring runoff but are warmer near the Kuroshio Current.

could be a result of fog/cloud processes that can deplete aerosol and sulfuric acid through uptake by cloud droplets [*Hegg and Hobbs*, 1981] while promoting nucleation in the near-cloud environment [*Clarke et al.*, 1999, 1998]. In section 5.1 we discuss the role of fog and the primary aerosol in depleting the number of recently formed secondary aerosols because of scavenging in a high-surface-area environment.

4.4. Profiles and Size Distributions Over the Kuroshio Current

[25] In order to interpret aerosol aging during transport it is important to recognize processes that influence the vertical distribution of aerosol during advection through the region. Figure 2 shows the air mass sampled during the southern profile of ACE-Asia flight 8 did not encounter land but passed over the warm waters of the Kuroshio Current, a strong source of heat and water vapor (Figure 5). During flight 8 the C-130 completed two vertical profiles at 0700 UTC (1600 local time) near the LIDAR installation at Amami-Ohshima. Figures 6a–6c show that the MBL is well mixed to 1.7 km and the SO_2 concentrations have dropped from a column average 5 ppbv over the Yellow Sea to 1.4 ppbv over the Kuroshio. In Figure 6d we show the number size distribution from the surface to 3000 m. After 2 days of transport from source regions in mainland China newly formed secondary aerosols were present throughout the MBL. Particle concentrations are highest near the MBL inversion (1.7 km) where C_{binary} and $C_{ternary}$ reach their minimum values. The nucleation parameterizations demonstrate that the cold high-relative-humidity conditions near the MBL inversion (decreasing T with constant w) are the favored site for the formation of secondary aerosols. However, the near-constant value for the measured dry scattering coefficient indicates that ambient scattering and associated aerosol surface area will be a maximum at 1600 m in the high-RH environment. Hence, if nucleation were occurring equally throughout the column we would expect the secondary aerosol population to be preferentially scavenged aloft. Consequently, the higher concentrations and size of the aerosol aloft implies that it is the most active source region for particles present in the MBL.

5. Analysis

5.1. Nucleation Mechanism and Fog Formation Over the Yellow Sea

[26] The profiles and size distributions over the Yellow Sea show a shallow layer directly above the cool ocean surface with distinct thermodynamic and aerosol properties. We expect this high-relative-humidity layer to be the preferred site for new particle production. During the central profile of TRACE-P flight 14, volatile CN (VCN) and 3-8 nm particle concentrations are positively correlated to relative humidity until an altitude of $\sim$ 500 m (prior to 0358 UTC in Figure 7). However, below 500 m the near-surface SO_2 and H_2SO_4 as well as volatile CN (VCN) are anticorrelated (R^2 = 0.827, 0.811 and 0.835) with respect to relative humidity. As the P3-B ascended during the northern profile (after 0422 UTC in Figure 7) particle concentrations and VCN once again become positively correlated to relative humidity. In order to explain the observations we require a mechanism that simultaneously depletes gas-phase precursors as well as total particle number. Additionally, the mechanism must also account for less neutralization of the accumulation mode aerosol near the surface (as described in section 4.3) compared to those observed in the size distributions above the developing MBL.

[27] We propose that gas-phase precursors are depleted near the surface and that the accumulation mode is less neutralized because of enhanced production of sulfates [*Hegg and Hobbs*, 1981] in fog forming over the cool coastal waters near China (Figure 5). Although particles are favored to form near the surface, as predicted by C_{binary} and $C_{ternary}$, few of the new particles survived scavenging by rapid coagulation in a fog environment where surface area may be several orders of magnitude higher than the drier environments sampled aloft. Alternatively the less numerous and smaller particles sampled near the surface could have formed after the dissipation of the fog [*Kerminen and Wexler*, 1994b] while those aloft formed earlier in an

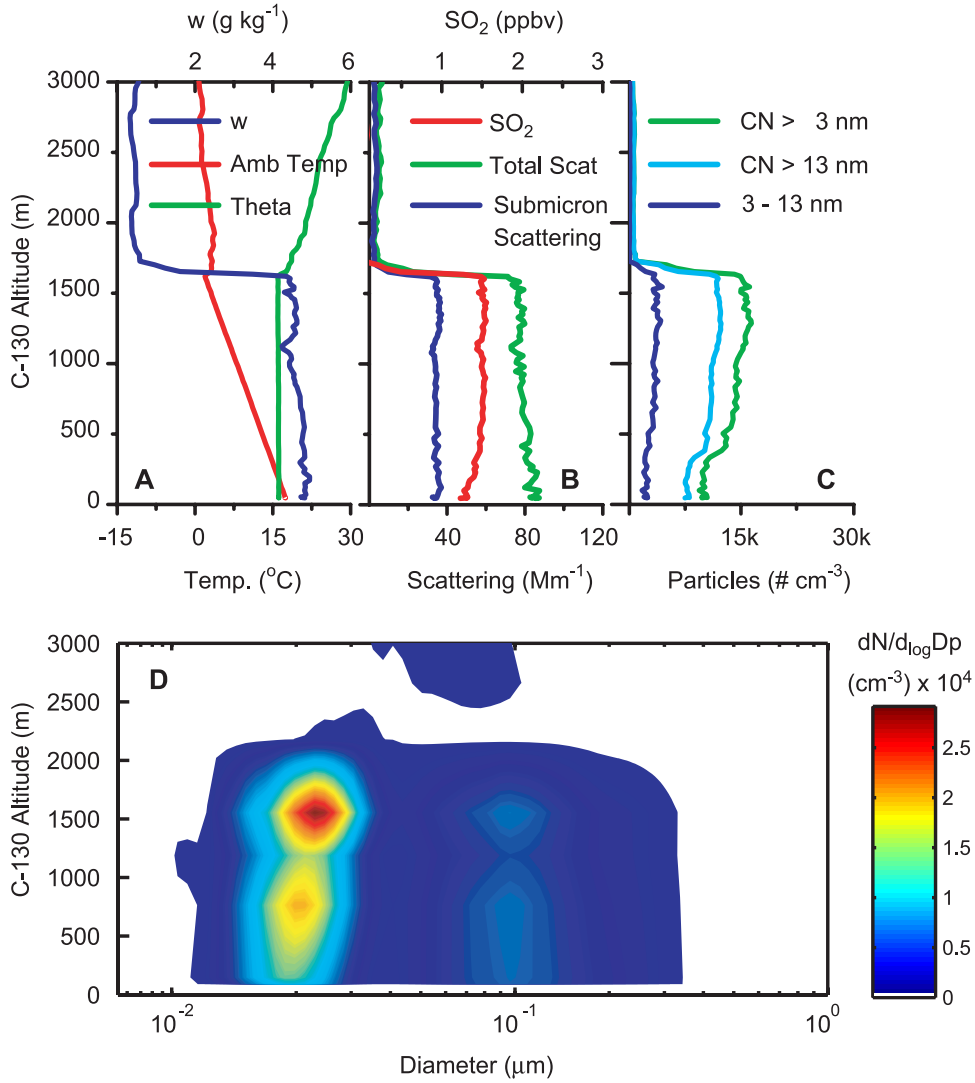

Figure 6. (a) Thermodynamic parameters, (b) SO_2 and light scattering, (c) and particle concentrations during the southern profile of ACE-Asia flight 8. (d) Vertical structure of aerosol number distributions at Amami-Ohshima during ACE-Asia flight 8. Warm waters of the Kuroshio Current appear responsible for the vertical mixing.

environment which favored their rapid condensational growth.

[28] If we extrapolate the values of water vapor mixing ratio and ambient temperature from 125 m during the level leg to the surface (25 m and 101.325 kPa), we can show that RH values for the southern and central TRACE-P flight 14 profiles exceed 100%. The crew aboard the NASA P3-B did not report fog over the Yellow Sea during the flight (18 March 2001). However, local meteorology stations did report "heavy fog," "fog," "smoke," and "haze" across the eastern and western (upwind) coasts of the Yellow Sea with reports extending past Shanghai to as far south as Hong Kong at 0000 UTC (0900 local time). One month later during ACE-Asia flight 7 (12 April) less extensive reports of "heavy fog," "smoke," "fog," and "haze" were recorded at coastal sites in the Yellow Sea and as far south as Shanghai although the crew aboard the NCAR C-130 did not report fog during the flight.

[29] For the TRACE-P flight 14 case calculations using the *Vehkamäki et al.* [2002] parameterization were made at 97% relative humidity (C_{binary} 97) to estimate the potential for binary nucleation under near cloud (fog) conditions. This is plotted along with the concentration of H_2SO_4 measured aboard the aircraft and C_{binary} at ambient conditions in the bottom panel of Figure 7. At 97% RH the parameterization approaches but still exceeds the observed concentration of H_2SO_4 by at least a factor of 5 although the model uncertainty is approximately 1 order of magnitude. Also, formation of secondary aerosols consumes gas-phase sulfuric acid such that concentrations measured after the aerosols have grown to detectable sizes could be lower than concentrations during gas to particle conversion.

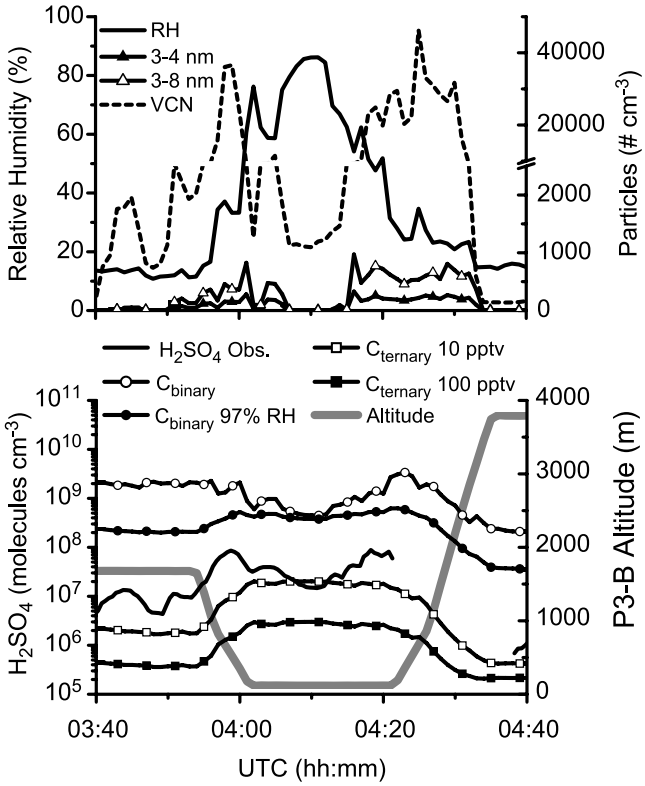

Figure 7. (top) Volatile CN (VCN), 3-4 nm, and 3-8 nm particle concentrations are anticorrelated to relative humidity below 500 m. Observed concentrations of sulfuric acid are generally insufficient to support binary nucleation (C_{binary}) under ambient conditions or when evaluated at 97% relative humidity (C_{binary} 97%). (bottom) Ternary parameterization ($C_{ternary}$) shows that nucleation rates of 10^5 s^{-1} are possible for ammonia concentrations as low as 10 or 100 pptv for the observed concentration of H_2SO_4.

[30] Also plotted in Figure 7 is the ternary parameterization of *Napari et al.* [2002c]. The curves presented are based on fixed concentrations of gas phase of ammonia (10 or 100 pptv), and a fixed nucleation rate, J, of 10^5 cm^{-3} s^{-1} under ambient conditions of temperature and RH. Typically nucleation rates of 10^0 cm^{-3} s^{-1} are considered significant [*Jaecker-Voirol and Mirabel*, 1989; *Vehkamäki et al.*, 2002]. In laboratory experiments, *Ball et al.* [1999] showed that 80 pptv of NH_3 (g) increases nucleation rates in the H_2SO_4, H_2O, NH_3 system by up to an order of magnitude at 15% RH. These findings are also consistent with models [*Kulmala et al.*, 2002; *Napari et al.*, 2002a, 2002b] and laboratory experiments [*Hanson and Eisele*, 2002] that show ammonia and sulfuric acid play a dominant role in forming new particles in the atmosphere. While the ternary parameterization is only valid up to NH_3 concentrations of 100 pptv, measurements in east Asia indicate that gas-phase ammonia concentrations typically exceed 1000 pptv [*Carmichael et al.*, 2003a; *Hong et al.*, 2002]. Simulations using the CFORS/STEM-2K3 model [*Carmichael et al.*, 2003c; *Tang et al.*, 2004] predict that the concentration of NH_3 for 18 March and 12 April along 124°E were in excess of 1000 pptv for the entire boundary layer (Figure 8).

[31] With only 100 pptv of NH_3 nucleation rates as high as 10^5 cm^{-3} s^{-1} are possible for 1 order of magnitude less H_2SO_4 than the concentrations measured aboard the aircraft. Since concentrations of gas-phase ammonia are likely as high as 1000 pptv it would appear that new particle production is a common occurrence in the region and that the new secondary aerosols were most likely forming via a ternary nucleation mechanism. Consequently, although new secondary aerosols may be forming near the surface, the presence of fog and and/or enhanced aerosol surface area due to relative humidity approaching 100% appears to dramatically reduce the formation, growth and survival of the newly formed secondary aerosols.

5.2. Nucleation Mode Growth Rates and Composition

[32] As mentioned in the introduction, surface measurements of particle nucleation and subsequent growth have been made at a number of sites in recent years [*Kulmala et al.*, 2004]. Surface sites during ACE-Asia also reported episodic events of new particle production. Intercomparison flights with the C-130 aircraft provide an opportunity to identify and explore the spatial and temporal features of some events in three dimensions. Nucleation/Aitken mode particles were observed throughout the developing MBL and pre-existing CBL on 12 April while traveling across 8 degrees of longitude (~720 km) and 4 degrees of latitude (~440 km). Moreover, while conducting operations in essentially the same air mass the following day the C-130 observed newly formed secondary aerosols throughout the

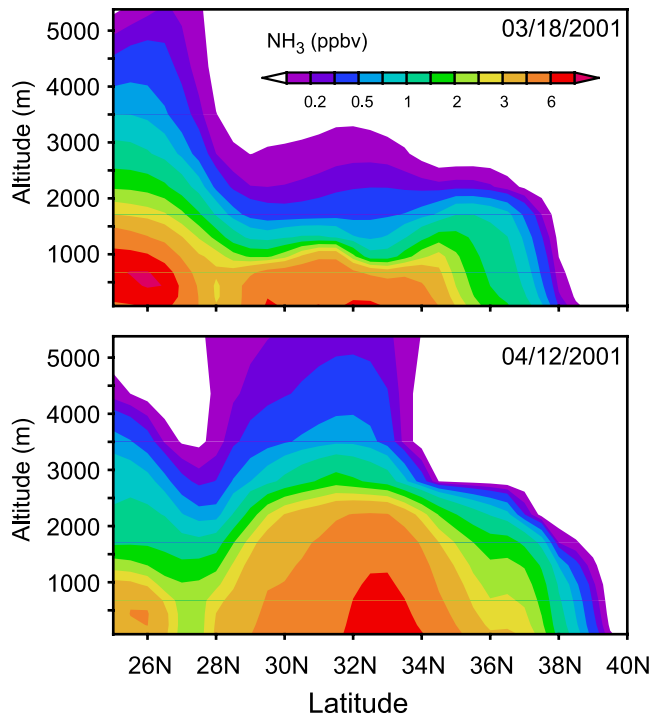

Figure 8. Simulated NH_3 concentrations from the CFORS/STEM-2K3 model (top) along 124°E during TRACE-P flight 14 and (bottom) along 124°E during ACE-Asia flight 7. Concentrations in the boundary layer typically exceed 1 ppbv, suggesting that gas-phase ammonia is available to participate in ternary nucleation with sulfuric acid and water.

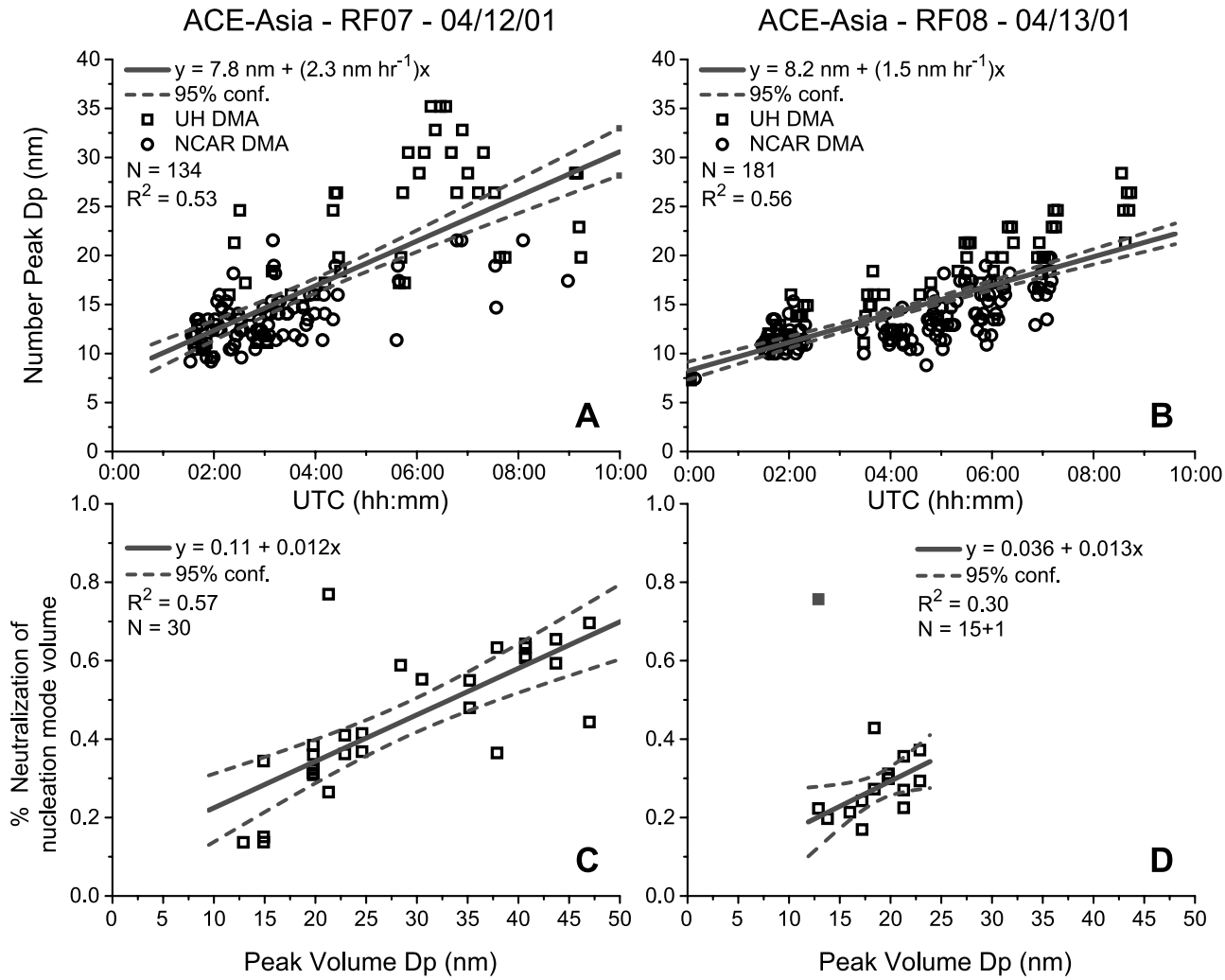

Figure 9. Linear regressions of nucleation/Aitken mode particle growth rates measured aboard the C-130 (a) over the Yellow Sea during ACE-Asia flight 7 and (b) north and south of Japan during ACE-Asia flight 8. (c and d) Degree of neutralization of the sulfuric-acid-dominated nucleation/Aitken mode aerosols versus the mode nucleation/Aitken diameter for ACE-Asia flights 7 and 8. Increasing neutralization as the particles grow indicates the condensation of ternary species such as NH_3 and possibly low-vapor-pressure organics.

MBL while covering 6 degrees of longitude (~540 km) and 7 degrees of latitude (~770 km). These observations show that formation of secondary aerosols occurred on a scale of ~200,000 km^2 over a 2-day period in a fairly homogeneous air mass. The growth of these nuclei for ACE-Asia flights 7 and 8 were regionally characterized (Figures 9a and 9b) by plotting the peak diameters of the recently formed secondary aerosols versus UTC time of the C-130 observations. The graphs show similar growth rates of 2.3 and 1.5 nm h^{-1} for the flights with R^2 statistics of 0.53 and 0.56. These values are consistent with other observed growth rates [*Aalto et al.*, 2001; *Birmili and Wiedensohler*, 2000; *Birmili et al.*, 2000; *Stratmann et al.*, 2003; *Verheggen and Mozurkewich*, 2002; *Weber et al.*, 1997, 1998a]. The data show a slightly higher growth rate in the Yellow Sea (flight 7) as compared to the Sea of Japan and East China Sea (flight 8) despite the presence of high aerosol surface area (up to 1200 μm^2 cm^3) due to anthropogenic pollution and mineral dust. Intercepts for both growth plots suggest that at 0000 UTC (0900 local time) the particles had sizes of ~8 nm. If nucleation commenced shortly after sunrise (0611 and 0613 local time), particle growth rates early in the day must have been slightly faster than those observed later by the C-130. Growth is also evident in the evolving size distributions measured on 12 April by the Gosan surface site and on 13 April aboard the R/V *Ron Brown* (Figure 10). The growth rate equation calculated from the C-130 data is plotted in Figure 10 and appears consistent with those measured for the remainder of each day at the surface sites. These observations demonstrate that particle formation and growth occurred on a synoptic scale over the 2-day period and that the C-130 aircraft sampled an exceptionally homogeneous air mass in a quasi-Lagrangian fashion.

[33] Size distributions measured at 150°C are also of interest since they appear related to neutralization of sulfuric acid species [*Clarke et al.*, 1998]. Figures 9c and 9d show the ratio of nucleation/Aitken mode volume at 150°C to

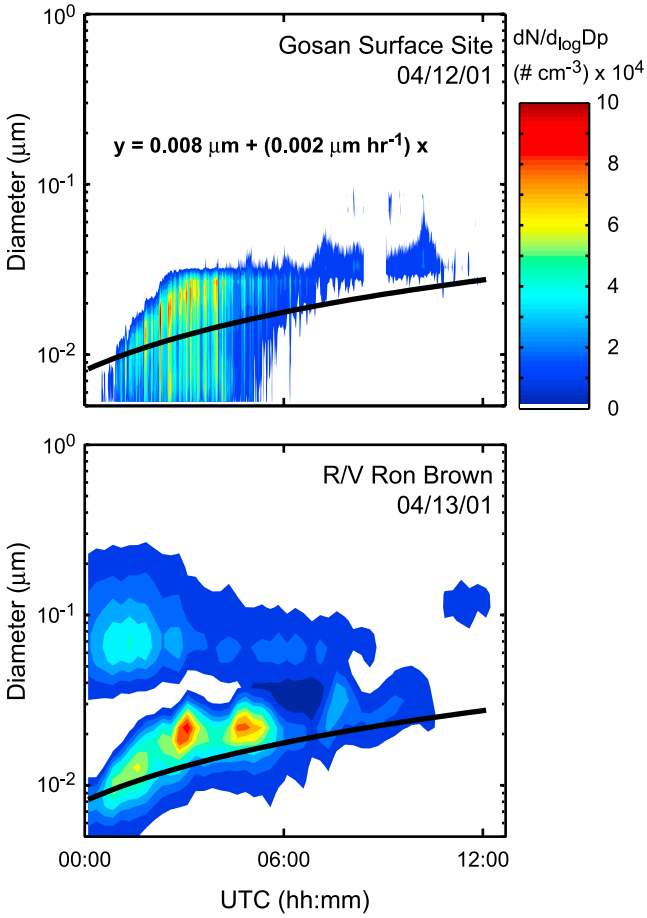

Figure 10. Evolution of the newly formed secondary aerosols as (top) observed at the Gosan surface site on 12 April and (bottom) observed by the R/V *Ron Brown* on 13 April. Surface growth rates are broadly consistent with the linear regression of growth rates calculated from the C-130 size distributions while surveying the regional air mass aloft (Figures 9a and 9b).

nucleation/Aitken mode volume at dry ambient conditions plotted versus the peak diameter of the dry ambient mode. Ratios near one can represent an ammonium bisulfate or ammonium sulfate type composition while a ratio of zero would indicate pure sulfuric acid. While inferring the composition of the critical cluster (i.e., the nucleating particle) from the composition of 10–25 nm particles is highly uncertain, the reduced volatility at 150°C with time implies the newly formed secondary aerosols were becoming increasingly neutralized over time. Additional evidence for the presence of ammonia in the newly formed aerosols comes from the Gosan surface site on 12 April. Using a humidified tandem differential mobility analyzer (HTDMA), the research group from Brookhaven National Laboratory determined that the hygroscopic growth of 25 nm particles was best explained by an ammonium sulfate/ammonium bisulfate type composition. This also suggests a ternary mechanism involving ammonia (and possibly low-vapor-pressure organics) rather than binary nucleation for the formation of the secondary aerosols. Additionally, the participation of ternary acid species such as HNO_3 and MSA can probably be ruled out under the prevailing conditions of RH, T, NH_3 and H_2SO_4 [*Napari et al.*, 2002a]. During the TRACE-P case the nucleation/Aitken mode aerosols did not appear to be significantly neutralized indicating that sulfuric acid was the dominant condensing species. Under the TRACE-P conditions of temperature and relative humidity, C_{binary} shows that binary nucleation may have been possible during morning fog. However, under the expected concentrations of ammonia (>1 ppbv; Figure 8) it is probable that a ternary mechanism was responsible for the new particle production while the dominant condensing species was sulfuric acid.

5.3. Flux Rate of Sulfuric Acid to the Size Distribution

[34] Using the change of particle diameter with respect to time, dD_p/dt, we can calculate the condensation sink (CS) by adopting the method of *Kulmala et al.* [2001a]. This calculation will allow us to estimate the flux rate of vapor (believed to be dominated by sulfuric acid) to the size distribution.

The differential equation

$$\frac{dC}{dt} = Q - \mathrm{CS} \cdot C \tag{2}$$

can be evaluated assuming production and removal of sulfuric acid is in quasi-steady state. That is to say that $dC/dt = 0$, where Q is the vapor formation rate, C is the vapor concentration, and CS is the condensational sink. The growth rate of the particles is given by

$$\frac{dD_p}{dt} = \frac{2m_v \beta_m D_v C}{\rho D_p}, \tag{3}$$

where m_v is the molecular mass of the condensable sulfuric acid vapor (98.08 g mol^{-1}). The diffusivity of the sulfuric acid vapor in air is D_v, ρ is the particle density (assumed to be 1.4 g cm^{-3} for H_2SO_4), assuming $\alpha = 1$ as the mass accommodation coefficient and where β_{mi} is the transitional correction factor for mass flux integrated over the size distribution and is a function of the Knudsen number [*Seinfeld and Pandis*, 1998]. The condensational sink CS is expressed as $2\pi D_v \mathrm{CS}'$ where

$$\mathrm{CS}' = \sum_i \beta_{mi} D_{p_i} N_i. \tag{4}$$

[35] The values for the condensation sink (CS) terms and the vapor formation rates (Q) are summarized in Table 1. Growth rates of 2 nm h^{-1} were used on the basis of the regression in Figures 9a and 9b. These growth rates were then applied to three size distributions from TRACE-P flight 14, five size distributions from ACE-Asia flight 7 and three distributions from ACE-Asia flight 8. The mean vapor flux using a quasi-steady state assumption (assuming $Q = \mathrm{CS} \cdot \mathrm{C}$) is 2.3×10^6 molecules cm^{-3} s^{-1} $\pm 1.1 \times 10^6$ molecules cm^{-3} s^{-1}. This value is within a factor of 2 or 3 of sulfuric acid production rates of 1.0×10^6 molecules cm^{-3} s^{-1} calculated by *Weber et al.* [2003] for TRACE-P flight 14. Such close agreement between the two calculations suggests that concentrations of sulfuric acid alone can account for the observed particle growth

Table 1. Sulfuric Acid Flux Rate to Aerosol Size Distributions Measured During TRACE-P Flight 14 on 18 March 2001 and ACE-Asia Flights 7 and 8 on 12 and 13 April 2001

Flight	Time, UTC	Altitude, m	SA, $\mu m^2\ cm^{-3}$	dD_p/dt, nm h^{-1}	CS, s^{-1}	Q, molecules $cm^{-3}\ s^{-1}$
TP RF14	0353–0400	663	644	2	3.8E-02[a]	3.3E+06
	0403–0415	118	1221	2	3.6E-02	3.2E+06
	0419–0425	155	1144	2	4.9E-02	4.3E+06
AA RF07	0136–0145	97	690	2	1.8E-02	1.6E+06
	0409–0412	48	774	2	2.1E-02	1.8E+06
	0419–0422	677	609	2	3.8E-02	3.4E+06
	0542–0544	512	667	2	2.8E-02	2.5E+06
	0700–0708	50	747	2	2.3E-02	2.0E+06
AA RF08	0148–0205	61	426	2	1.5E-02	1.3E+06
	0659–0701	93	389	2	1.3E-02	1.1E+06
	0712–0714	1295	295	2	1.1E-02	9.8E+05
Mean					2.6E-02	2.3E+06
SD[b]					1.2E-02	1.1E+06

[a]Read 3.8E-02 as 3.8×10^{-2}.
[b]SD, standard deviation.

with the slightly higher value possibly a result of condensing ternary species such as ammonia or organics.

6. Discussion

[36] Ground based measurements in northern Europe have shown that synoptic-scale secondary aerosol formation can occur in postfrontal conditions associated with cold air outbreaks of polar or arctic air masses [*Kulmala et al.*, 2001b; *Nilsson et al.*, 2001]. In these cases marine air is making the transition to a continental air mass. Off the coast of Asia our observations show synoptic-scale postfrontal secondary aerosol formation as the air mass makes a transition from dry continental conditions to moist marine conditions under the prevailing offshore flow during spring. Highest concentrations of secondary aerosol appear to be associated with steep vertical gradients in aerosol surface area, relative humidity and temperature at the interface between the developing MBL and the pre-existing continental boundary layer (Figure 3). Our observations appear to confirm hypotheses in other publications [*Easter and Peters*, 1994; *Nilsson and Kulmala*, 1998] that suggest that nucleation events can occur in regions where mixing of air masses can result in conditions that lead to supersaturations of the condensable species (e.g., fluctuation in relative humidity, temperature, H_2SO_4, SO_2, aerosol surface area etc.).

[37] Observations over the Yellow Sea during TRACE-P and ACE-Asia indicate that cooler conditions prevailed early in the day and formation of fog enhanced the transfer of gas-phase precursors to the aerosol size distribution. Within and directly above the fog layer, a binary and/or ternary nucleation mechanism created the high concentrations of newly formed secondary aerosols. This formation mechanism is also consistent with the postfog nucleation of *Kerminen and Wexler* [1994b] and similar to conditions associated with nucleation near cloud outflow [*Clarke et al.*, 1999, 1998; *Weber et al.*, 2001a]. Although high RH and colder temperatures may create more favorable conditions for nucleation of sulfuric acid aerosol, if these conditions lead to fog or cloud formation then the increase in surface area both scavenges gas-phase precursors and many of the nuclei formed. It is clear the production and growth of nuclei will vary greatly in the region even when precursors remain at similar levels. Hence part of the reason nucleation was not always evident under otherwise similar pollution outflow may be related to its scavenging by fog or cloud common to the region in the spring [*Chung et al.*, 1999].

6.1. Regional Aerosol and Their Link to Springtime Meteorology

[38] The R/V *Ron Brown* traveled from Tokyo, then south of Japan and into the Sea of Japan before returning along the same route between 1 April and 22 April 2001. Rawinsondes launched from the ship during the cruise showed the passage of four major frontal systems between 1 April and 16 April. Broadly classifying the ship-based measurements into ''prefrontal,'' ''frontal,'' and ''postfrontal'' meteorological conditions illustrates the differences in aerosol composition under these meteorological situations (Table 2). Wind direction is predominantly offshore flow from the west during the frontal and postfrontal conditions while flow is generally from the SE during prefrontal conditions and reflects the recirculation of the warm sector air onshore toward the next advancing front approaching from the NW [*Fuelberg et al.*, 2003; *Hannan et al.*, 2003; *Liu et al.*, 2003]. Total aerosol number (>3 nm) and SO_2 concentrations during prefrontal and frontal conditions are broadly similar and associated with high relative humidity and some precipitation. Median and mean values of total aerosol number and nucleation mode (3–13 nm) particles concentrations between 0600 and 1500 local time show that there is a background of nucleation mode particles during prefrontal and frontal activity and indicative of stable populations in this heavily impacted region under all meteorological conditions. During postfrontal conditions low relative humidity, high solar insolation and lack of rainfall indicate cloud-free conditions during subsidence. During postfrontal activity median values of total and nucleation mode particle number are nearly double the background conditions but much higher mean values are indicative not only of the explosive nature of new particle production during these episodic events but also suggest rapid depletion of new particle number throughout the day due to coagulation. SO_2 concentrations during postfrontal

Table 2. Summary of Aerosol and Meteorological Parameters Measured Aboard the R/V *Ron Brown* Between 1 April and 16 April During "Prefrontal," "Frontal," and "Postfrontal" Air Mass Types as Determined From Ship-Based Rawinsonde Data[a]

	CN > 3 nm, # cm^{-3}	CN 3–13 nm, # cm^{-3}	SO_2, ppbv	RH, %	Average Solar Insolation for Period, W m^{-2}	Wind Speed, m s^{-1}	Wind Direction, deg	Rain Rate, mm h^{-1}
				Prefrontal (49% of Cases)				
Median	3661	608	0.72	84	610	4.1	109	0.00
Mean	3622	626	2.32	78	540	4.3	115	0.02
SD	977	185	3.55	14	286	1.8	52	0.29
				Frontal (21% of Cases)				
Median	3031	452	0.82	78	229	7.8	237	0.00
Mean	3208	462	1.15	76	244	8.0	236	0.42
SD	1724	198	0.98	9	167	2.8	91	1.40
				Postfrontal (30% of Cases)				
Median	4926	1026	0.78	53	748	8.7	264	0.00
Mean	12,274	5500	1.51	53	630	8.2	216	0.00
SD	13,131	7654	1.40	4	326	3.1	110	0.01

[a]Data have been selected between 0600 and 1500 local time to highlight the event-based nature of secondary aerosol formation under relatively dry, cloud-free conditions in the postfrontal air masses.

conditions are indistinguishable between each of the meteorological situations indicating it is not only gas-phase precursor concentrations that influence regional concentrations of new particles.

6.2. Spatial Distribution of Primary and Secondary Aerosols

[39] Flight paths (Figure 1) can be biased by various experimental objectives and are limited temporally and spatially. Because observations based on new particle production were not an experimental objective we assume that these events are random and representative. In spite of extensive evidence of nucleation discussed above, Figure 1 shows that significant nucleation events were limited and typically confined below 2000 m and north of 25°N. Primary emissions with little evidence of widespread secondary aerosol formation are more frequent but generally lower in total aerosol concentration. Hence it is of interest to examine the relative contributions of primary and secondary aerosol to the regional export of aerosol. In order to analyze the newly formed secondary aerosols in the context of the regional background we have further divided the data east and west of 130°E. The demarcation along 130°E roughly divides the data into air masses <24 hours old (those west of 130°E) and those >24 hours (east of 130°E) on the basis of back trajectories (Figure 2) under the prevailing offshore flow [*Jordan et al.*, 2003]. In each of the five cases listed below we have also removed periods of data where SO_2 concentrations exceeded 10 ppbv in order to eliminate air masses that were heavily impacted by regional volcanic emissions. The case studies are classified A through E according to the following: A, west nucleation (altitude < 2 km, latitude > 25°N, longitude < 130°E); B, east nucleation (altitude < 2 km, latitude > 25°N, longitude > 130°E); C, west no-nucleation (altitude < 2 km, latitude > 25°N, longitude < 130°E); D, east no-nucleation (altitude < 2 km, latitude > 25°N, longitude > 130°E); E, southern data (altitude < 2 km, latitude < 25°N).

[40] Table 3 shows the median, mean, standard deviations and trimmed mean (top and bottom deciles removed) of 1-min data for the CO enhancement (CO with an assumed background of 60 pptv removed), RCN (# cm^{-3}), SO_2 (pptv) and VCN (# cm^{-3}) for these five regional classifications. CO is a conservative tracer for combustion while RCN is a conservative measure of primary aerosols dominated by soot that become internally mixed with components like sulfate and organic carbon (OC) [*Clarke et al.*, 2004]. SO_2 is not conservative as it is consumed in photochemical processes and deposition to surfaces. We believe that most VCN are a measure of the recently nucleated secondary aerosols (VCN_{sec}) but may also include volatile particles formed in or near the source emissions. Such VCN would also be primary (VCN_{pri}) and distinct from newly formed secondary aerosols discussed in this paper. Later we will examine the implications of primary and secondary emissions by allowing that the actual secondary aerosol VCN_{sec} might range between the measured VCN and VCN-VCN_{pri}, where the latter is described below. First we make the following observations based primarily on the behavior of median values in Table 3: (1) Comparable flight time (~2500 min or 42 hours) was spent both east and west of 130°E and below 2000 m. (2) Significant nucleation events occurred ~1/3 of the time both east and west of 130°E. (3) West of 130°E, nucleation events (case A) were associated with primary aerosol (RCN) and SO_2 enhanced by a factor of ~2.5 over nonnucleation events (case C) while enhanced CO was only 30% higher, indicative of SO_2's involvement in the phenomenon. (4) West of 130°E, nucleation events (case A) had median secondary aerosol concentrations (VCN) an order of magnitude larger than nonnucleation events (case C) and with much higher mean and standard deviations reflecting their variability. (5) East of 130°E, nucleation events (case B) show a drop in both median and mean VCN by a factor of 2 from those in the west (case A) even though primary RCN and SO_2 drop by only 20% and 10%, respectively. This indicates that the aged VCN from the previous day and any new VCN freshly nucleated are typically far fewer in total number than VCN formed on the first day of transport from the Asian mainland. (6) Nonnucleation events east and west of 130°E have similar primary RCN and VCN indicting little depletion as the air mass ages. (7) Data south of 25°N (TRACE-P)

Table 3. Campaign-Wide Statistics of CO Enhancement (CO − 60-pptv CO), Refractory CN (RCN), SO_2, and Volatile CN (VCN) During the ACE-Asia and TRACE-P Experiments During Spring of 2001[a]

Statistic	CO Enhancement, pptv	RCN, # cm^{-3}	SO_2, pptv	VCN, # cm^{-3}
A: Nucleation Events West of 130°E				
Median	241	4159	1810	5451
Mean	282	4296	2432	10,699
SD	128	1611	1853	11,866
Trimmean (10%)	267	4225	2174	8647
N	737	859	951	859
B: Nucleation Events East of 130°E				
Median	155	3346	1659	2689
Mean	167	3493	1845	5794
SD	62	1542	1390	8393
Trimmean (10%)	161	3414	1693	3737
N	637	874	1074	874
C: Nonnucleation Events West of 130°E				
Median	165	1735	593	321
Mean	179	1933	748	484
SD	89	1159	777	485
Trimmean (10%)	168	1829	617	385
N	1372	1646	1818	1646
D: Nonnucleation Events East of 130°E				
Median	135	1597	337	349
Mean	139	1720	709	802
SD	57	1219	1147	1160
Trimmean (10%)	136	1600	470	518
N	1365	1773	1958	1773
E: TRACE-P Data South of 25°N				
Median	80	335	71	151
Mean	108	762	107	145
SD	77	770	121	101
Trimmean (10%)	94	647	82	128
N	940	922	986	922

[a]RCN, refractory CN; VCN, volatile CN. Regions are classified on the basis of the 1-min aircraft data sets according to nucleation (CN 3–13 nm > 1000 cm^{-3}) and nonnucleation event periods, west and east of 130°E, north and south of 25°N, and below 2-km flight altitude. Air masses influenced by volcanic emissions (SO_2 > 10 ppbv) have been eliminated.

indicate values far lower in all parameters compared to those in the north. The biomass plumes in the south were typically transported over the Pacific at altitudes above 2 km [*Clarke et al.*, 2004] and are much lower in SO_2 resulting in less frequent nucleation events (see also Figure 1).

[41] In summary, significant nucleation events occurred regionally only ~33% of the time but were most pronounced north of 25°N and in air masses most recently exposed to the highest combustion sources and SO_2 (Figure 1). Although nucleation was ongoing during the second day of transport out over the coastal bodies of water, the "new" volatile nuclei (VCN) were only about half of those present on the first day and are reduced relative to the other aerosol and gas components. This is presumed to reflect a combination of aging, coagulation (in and out of cloud) combined with typically weaker net production on the second day. We note that significant VCN are present in the nonnucleation cases and these are also higher than the values south of 25°N.

[42] By assuming that all volatile CN north of 25°N are newly produced secondary aerosols we can calculate the relative contribution of the secondary aerosols to the total aerosol population over the two month observations period where f_A (0.34) and f_B (0.33) are the frequency of the nucleation events (west and east of 130°E) according to

$$\frac{\text{SECONDARY}_{\text{West}}}{\text{TOTAL}_{\text{West}}} = \frac{\text{VCN}_A}{\text{RCN}_A + \text{VCN}_A} f_A + \frac{\text{VCN}_C}{\text{RCN}_C + \text{VCN}_C}(1 - f_A), \quad (5)$$

$$\frac{\text{SECONDARY}_{\text{West}}}{\text{TOTAL}_{\text{West}}} = \frac{5451}{4159 + 5451} \cdot 0.34 + \frac{321}{1735 + 321} \cdot (1 - 0.34) = 30\%.$$

[43] Using the values from Table 3, we see that 30% of the springtime aerosol population consists of secondary aerosols west of 130°E, and 27% of the population consists of secondary aerosol east of 130°E.

[44] Alternately, some of the measured VCN may be natural (e.g., entrainment from free troposphere) and some may be formed along with primary soot aerosol as VCN_{pri} in or near combustion plumes. In the latter case, it is possible that the primary VCN in cases A and B trend with the primary RCN. Hence, as an alternative to assuming all VCN are secondary we can estimate VCN arising from nucleation alone (VCN_{sec}) by scaling VCN_{pri} with the RCN assuming the ratio (VCN_{pri}/RCN) for the nonnucleation cases will also hold for the nucleation cases, as show in equation (6).

$$\text{VCN}_{\text{pri\_}A} = \left(\frac{\text{RCN}_A}{\text{RCN}_C}\right) \cdot \text{VCN}_{\text{pri\_}C},$$
$$\text{VCN}_{\text{pri\_}A} = \left(\frac{4159}{1735}\right) \cdot 321 = 769 \text{ cm}^{-3}. \quad (6)$$

[45] The resulting VCN_{pri_A} estimated for the nucleation cases can then be subtracted from the total VCN such that

$$\text{VCN}_{\text{sec\_}A} = \text{VCN} - \text{VCN}_{\text{pri\_}A},$$
$$\text{VCN}_{\text{sec\_}A} = 5451 - 769 = 4681 \text{ cm}^{-3}. \quad (7)$$

[46] Under this assumption, VCN_{pri} represent 14 and 12% of the total VCN during the nucleation events (west and east) and are substantially above the global estimate of 3% used by *Adams and Seinfeld* [2003]. We can use the values of VCN_{pri}, VCN_{sec} and RCN to calculate the relative contribution of secondary aerosols to the total aerosol population according to

$$\frac{\text{SECONDARY}}{\text{TOTAL}_{\text{CN}}} = \frac{\text{VCN}_{\text{sec}}}{\text{RCN} + \text{VCN}_{\text{pri}} + \text{VCN}_{\text{sec}}},$$
$$\frac{\text{SECONDARY}}{\text{TOTAL}_{\text{CN}}} = \frac{4681}{4159 + 769 + 4681} = 49\%. \quad (8)$$

[47] Thus, during identified nucleation events newly formed secondary aerosols from the source regions in Asia represent 49% and 32% of the total aerosol population after approximately 24 hours (Yellow Sea) and 48 hours (over Japan) of transport (respectively). Nucleation events occurred west of 130°E thirty-four percent of the time (f_A = 0.34) and east of 130°E thirty three percent of the time (f_B = 0.33). The frequency of events recorded by the aircraft is

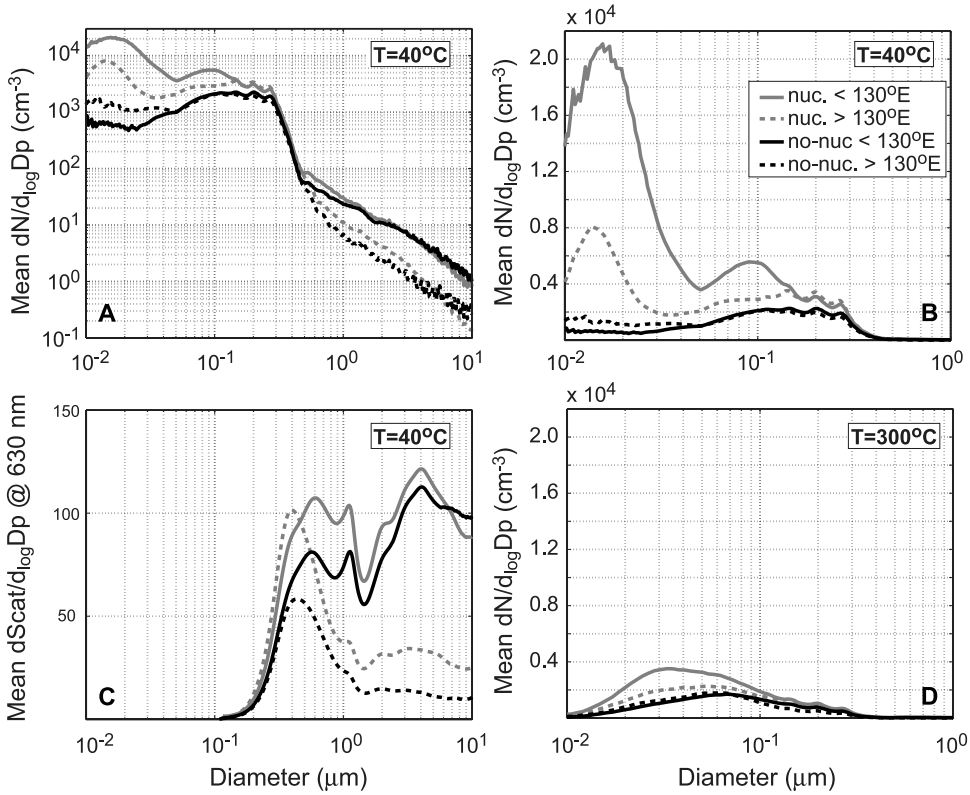

Figure 11. Mean aerosol distributions during nucleation (gray) and nonnucleation (black) events west (solid curves) and east (dashed curves) of 130°E during the ACE-Asia and TRACE-P campaigns displayed as (a) log-log and (b) semilog number distributions. (c) Scattering distribution (λ = 630 nm) calculated from the number distributions. (d) Refractory aerosol distributions preheated to 300°C.

close to the 30% frequency of nucleation events, such as 13 April (bottom of Figure 10), recorded by the R/V *Ron Brown*. The events recorded by the *Ron Brown* were linked to the occurrence of postfrontal air masses in Table 2. Variable winds due to island effects make interpretation of the Gosan meteorology more difficult (K. Bower, personal communication, 2003). However, the surface site observed an elevated background of nucleation mode particles 82% of the time and strong, episodic nucleation, such as those measured on 12 April (top of Figure 10) and 13 April, 36% of the time. Merging these results with the nonevent cases we can estimate a spring seasonal average (March and April 2001) for their contribution to the regional aerosol. Using two different assumptions about VCN, we conclude that newly produced secondary aerosols derived from anthropogenic emissions should range between 10% and 30% of the total aerosol population off the coast of Asia after 2 days of transport. Consequently, in spite of frequent and significant nucleation events it is the primary aerosols that constitute 70–90% of the total number of regional springtime aerosol emissions being advected out over the North Pacific in the marine boundary layer.

6.3. Mean Size Distributions of Primary and Secondary Aerosols

[48] It is also revealing to examine the mean size distributions associated with the above five classifications. We select the mean rather than the median so that the extreme nucleation cases are included. The median values, though arguably more regionally representative, tend to be lower thus minimizing the impact of the secondary aerosol population relative to the primary aerosols. Composite aerosol size distributions using the airborne rDMA and OPC systems aboard the P3-B and C-130 were separated on the basis of the same criteria as the stratification described in section 6.2.

[49] Dry ambient aerosol size distributions for the nucleating cases (Figures 11a and 11b: log-log and semilog, respectively) are consistent with the measurements described in Table 3 and show nucleation/Aitken mode particle concentrations in these cases are up to an order of magnitude more numerous than the so-called "nonnucleation cases" identified earlier. However, the composite size distributions also reveal that there are identifiable nucleation and Aitken mode particles even in cases where their low concentrations classified them as "nonnucleation" events. This indicates that the region commonly experiences some new particle production but most of the time the nucleation is either far less productive or the new particle number are being suppressed during initial growth through removal processes such as coagulation in clouds or fog.

[50] For the mean "nucleation event" size distributions, approximately half of the nucleation/Aitken mode particle volume for particles smaller than 0.04 μm remains after heating to 150°C. This type of volatility is consistent with partial neutralization of sulfuric acid to ammonium bisulfate or ammonium sulfate as shown in Figures 9c and 9d. Size distributions heated to 300°C (Figure 11d) show nuclei

smaller than 0.04 μm are completely removed and that concentrations of refractory primary aerosols are also greater during the nucleation events than during nonevent periods. This is also consistent with the high pollution emissions being enriched both in refractory black carbon and SO_2 (Figure 1 and Table 3). Moreover, the peak in the unheated number mode near 0.1 μm (Figure 11b) is reduced in diameter by a factor of ~5 upon heating (Figure 11d) with smallest sizes showing the greatest shift. The heated accumulation mode integral number (area under curve in Figure 11d) is little changed from the unheated accumulation mode (Figure 11b). This is consistent with this refractory component being black carbon (BC) having ~5–15% of the accumulation mode mass that is internally mixed with volatile condensed species [*Clarke et al.*, 2004]. Hence, after 2 days of transport, dry particle sizes larger than ~0.060 μm have few (less than ~10%) of their number that can be identified as secondary aerosol retaining the volatile properties of the original nucleation events.

[51] The significance of aerosol evolved from nucleation events to radiative forcing can be inferred from plots of the scattering distributions (λ = 630 nm) for the four cases shown in Figure 11c. Negligible contributions to total scattering exist for sizes below 0.200 μm even if these were humidified to ambient conditions. Relative to the primary aerosol the number of secondary aerosols is insignificant for sizes above 0.200 μm and implies that radiative effects of aerosol emissions from this region will not be affected by secondary particle formation but will be determined exclusively by primary emissions (including dust and sea salt) and the species that condense upon them.

7. Conclusions

[52] The ACE-Asia and TRACE-P aircraft observations provided the opportunity to study aerosol nucleation and growth over broad spatial and vertical scales. Investigations in two postfrontal air masses revealed widespread nucleation occurring over 200,000 km^2. These and other cases of enhanced nucleation were mostly confined within the boundary layer downwind of major Asian pollution sources emitting the gas-phase nucleation precursors SO_2 and NH_3. Thermal volatility of the nucleation mode particles often suggested sulfuric acid or a partially neutralized sulfuric acid species although organic carbon species could be a contributor. Parameterization of binary nucleation [*Vehkamäki et al.*, 2002] indicates that the observed concentrations of sulfuric acid were generally too low to produce new particles except possibly within and/or directly above morning fog confined below 600 m over the Yellow Sea. The ternary nucleation parameterization of *Napari et al.* [2002c] shows that under the observed concentration of sulfuric acid nucleation rates as high as 10^5 cm^{-3} s^{-1} were possible for ammonia concentrations of only 10 pptv. Although gas-phase ammonia was not measured, models and observations suggest concentrations in excess of 1000 pptv are common to the region.

[53] Growth rates of 2.3 nm h^{-1} and 1.5 nm h^{-1} for recently nucleated particles were inferred from the regional temporal size evolution of these distributions on 12 April and 13 April 2001. This growth was used to estimate flux rates of sulfuric acid to the aerosol size distribution of 2.3 ± 1.1×10^6 molecules cm^{-3} s^{-1}. This value is within about a factor of 2 of the estimated sulfuric acid production rates of 1.0×10^6 molecules cm^{-3} s^{-1} *Weber et al.* [2003] in this region during TRACE-P flight 14. Increasing neutralization of the nucleation mode aerosol over time suggests that other species are involved in the particle growth process but that sulfuric acid is an important and possibly dominant contributor to the aerosol production and growth in the aging urban plumes as they move out over the Pacific Ocean.

[54] The influence of fog and high RH was shown to dramatically reduce the formation, growth and survival of new nuclei. Consequently, unless vapor condensation rates remain high and conditions are favorable for new particle survival (i.e., cloud-free), newly formed secondary aerosols are unlikely to dominate the aerosol number as the polluted continental air masses move away from the Asian continent toward the Pacific Ocean. On the basis of the frequency of the episodic nucleation events under cloud-free conditions, compared to the more typical concentrations of newly formed secondary aerosols we found that these secondary aerosol account for only 10–30% of total aerosol number leaving the region over the period studied. Consequently, based upon these observations primary emissions are estimated to be 70–90% of the typical particle number emitted during springtime Asian outflow. Because many of the new particles are in sizes too small to be effective CCN this would place an upper limit on regional average contribution of secondary aerosol to CCN over the Pacific. Moreover, because few grow to sizes larger than ~0.1 μm their mass scattering efficiency is low relative to the primary emissions and their regional contribution to direct radiative impact is negligible compared to primary aerosol and their associated condensed species.

[55] These results are in contrast to the formation and evolution of secondary nuclei in the remote free troposphere. There, nucleation in cloud scavenged air followed by slow growth with low coagulation allows these nuclei to become significant contributors to both CCN and, at times, scattering extinction in clean unpolluted regions [*Clarke and Kapustin*, 2002]. Hence global modeling of aerosol processes related to radiative effects and even CCN may be able to ignore the role of secondary nucleation in highly polluted regions but not in "clean" regions such as the remote Pacific.

[56] **Acknowledgments.** The authors would like to thank the reviewers for their suggestions to improve the scientific content and readability of this manuscript. This research was completed under NASA grant NCC-1-416 and NSF grant ATM00-02070. Thank you to Tad Anderson and Sarah Doherty from the University of Washington for supplying us with the total and submicrometer scattering measured aboard the NCAR C-130. Thank you to Glen Sachse and Thomas Slate at NASA Langley and Teresa Campos, Sam Hall, and Ian Faloona at NCAR for supplying their CO data as well as Lynn Russell and the NCAR team for providing us with rDMA (NSF grant ATM-0408501) and CN data aboard the NCAR C-130. The authors would like to thank all the members of the ACE-Asia and TRACE-P team and Barry Huebert, Daniel Jacob, and James Crawford for their leadership during these campaigns. We would also like to thank the people of China, Korea, and Japan for hosting us during the intensive observation periods of the experiments. This is SOEST contribution 6389.

References

Aalto, P., et al. (2001), Physical characterization of aerosol particles during nucleation events, *Tellus, Ser. B*, *53*, 344–358.

Adams, P. J., and J. H. Seinfeld (2003), Disproportionate impact of particulate emissions on global cloud condensation nuclei concentrations, *Geophys. Res. Lett.*, *30*(5), 1239, doi:10.1029/2002GL016303.

Albrecht, B. A. (1989), Aerosols, cloud microphysics, and fractional cloudiness, *Science*, *245*, 1227–1230.

Anderson, T. L., and J. A. Ogren (1998), Determining aerosol radiative properties using a TSI 3563 integrating nephelometer, *Aerosol Sci. Technol.*, *29*, 57–69.

Anderson, T. L., et al. (1996), Performance characteristics of a high-sensitivity, three-wavelength, total scatter/backscatter nephelometer, *J. Atmos. Oceanic Technol.*, *13*, 967–986.

Ball, S. M., D. R. Hanson, F. Eisele, and P. H. McMurry (1999), Laboratory studies of particle nucleation: Initial results for H_2SO_4, H_2O, and NH_3 vapors, *J. Geophys. Res.*, *104*(D19), 23,709–23,718.

Birmili, W., and A. Wiedensohler (2000), New particle formation in the continental boundary layer: Meteorological and gas phase parameter influence, *Geophys. Res. Lett.*, *27*(20), 3325–3328.

Birmili, W., A. Wiedensohler, C. Plass-Dulmer, and H. Berresheim (2000), Evolution of newly formed aerosol particles in the continental boundary layer: A case study including OH and H_2SO_4 measurements, *Geophys. Res. Lett.*, *27*(15), 2205–2208.

Buzorius, G., U. Rannik, E. D. Nilsson, and M. Kulmala (2001), Vertical fluxes and micrometeorology during aerosol particle formation events, *Tellus, Ser. B*, *53*, 394–405.

Carmichael, G. R., et al. (2003a), Measurements of sulfur dioxide, ozone and ammonia concentrations in Asia, Africa and South America using passive samplers, *Atmos. Environ.*, *37*, 1293–1308.

Carmichael, G. R., et al. (2003b), Evaluating regional emissions estimates using the TRACE-P observations, *J. Geophys. Res.*, *108*(D21), 8810, doi:10.1029/2002JD003116.

Carmichael, G. R., et al. (2003c), Regional-scale chemical transport modeling in support of the analysis of observations obtained during the TRACE-P experiment, *J. Geophys. Res.*, *108*(D21), 8823, doi:10.1029/2002JD003117.

Chung, Y. S., H. S. Kim, and M. B. Yoon (1999), Observations of visibility and chemical compositions related to fog, mist and haze in South Korea, *Water Air Soil Pollut.*, *111*, 139–157.

Clarke, A. D. (1991), A thermo-optic technique for in-situ analysis of size-resolved aerosol physicochemistry, *Atmos. Environ., Part A*, *25*, 635–644.

Clarke, A. D., and V. N. Kapustin (2002), A Pacific aerosol survey: Part I. A decade of data on particle production, transport, evolution, and mixing in the troposphere, *J. Atmos. Sci.*, *59*(3), 363–382.

Clarke, A. D., J. L. Varner, F. Eisele, R. L. Mauldin, D. Tanner, and M. Litchy (1998), Particle production in the remote marine atmosphere: Cloud outflow and subsidence during ACE-1, *J. Geophys. Res.*, *103*(D13), 16,397–16,409.

Clarke, A. D., V. N. Kapustin, F. L. Eisele, R. J. Weber, and P. H. McMurry (1999), Particle production near marine clouds: Sulfuric acid and predictions from classical binary nucleation, *Geophys. Res. Lett.*, *26*(16), 2425–2428.

Clarke, A. D., W. G. Collins, P. J. Rasch, C. N. Kapustin, K. Moore, S. Howell, and H. E. Fuelberg (2001), Dust and pollution transport on global scales: Aerosol measurements and model predictions, *J. Geophys. Res.*, *106*(D23), 32,555–32,569.

Clarke, A. D., et al. (2004), Size distributions and mixtures of dust and black carbon aerosol in Asian outflow: Physiochemistry and optical properties, *J. Geophys.*, *109*, D15S09, doi:10.1029/2003JD004378.

Easter, R. C., and L. K. Peters (1994), Binary homogeneous nucleation: Temperature and relative humidity fluctuations, nonlinearity, and aspects of new particle production in the atmosphere, *J. Appl. Meteorol.*, *33*, 775–784.

Eisele, F. L., and D. J. Tanner (1993), Measurement of the gas phase concentration of H_2SO_4 and methane sulfonic acid and estimates of H_2SO4 production and loss in the atmosphere, *J. Geophys. Res.*, *98*(D5), 9001–9010.

Fuelberg, H. E., C. M. Kiley, J. R. Hannan, D. J. Westberg, M. A. Avery, and R. E. Newell (2003), Meteorological conditions and transport pathways during the Transport and Chemical Evolution over the Pacific (TRACE-P) experiment, *J. Geophys. Res.*, *108*(D20), 8782, doi:10.1029/2002JD003092.

Hannan, J. R., H. E. Fuelberg, J. H. Crawford, G. W. Sachse, and D. R. Blake (2003), The role of wave cyclones in transporting boundary layer air to the free troposphere during the spring 2001 NASA/TRACE-P experiment, *J. Geophys. Res.*, *108*(D20), 8785, doi:10.1029/2002JD003105.

Hanson, D. R., and F. L. Eisele (2002), Measurement of prenucleation molecular clusters in the NH_3, H_2SO_4, H_2O system, *J. Geophys. Res.*, *107*(D12), 4158, doi:10.1029/2001JD001100.

Hanson, D. R., F. Eisele, S. M. Ball, and P. H. McMurry (2002), Sizing small sulfuric acid particles with an ultrafine particle condensation nucleus counter, *Aerosol Sci. Technol.*, *36*, 554–559.

Hegg, D. A., and P. V. Hobbs (1981), Cloud water chemistry and the production of sulfates in clouds, *Atmos. Environ.*, *15*, 1597–1604.

Hong, Y.-M., B.-K. Lee, K.-J. Park, M.-H. Kang, Y.-R. Jung, D.-S. Lee, and M.-G. Kim (2002), Atmospheric nitrogen and sulfur containing compounds for three sites of South Korea, *Atmos. Environ.*, *36*, 3485–3494.

Huebert, B. J., T. Bates, P. B. Russell, G. Shi, Y. J. Kim, K. Kawamura, G. Carmichael, and T. Nakajima (2003), An overview of ACE-Asia: Strategies for quantifying the relationships between Asian aerosols and their climatic impacts, *J. Geophys. Res.*, *108*(D23), 8633, doi:10.1029/2003JD003550.

Intergovernmental Panel on Climate Change (2001), *Third Assessment Report: Climate Change 2001*, edited by D. L. Albritton and L. G. M. Filho, Cambridge Univ. Press, New York.

Jacob, D. J., J. H. Crawford, M. M. Kleb, V. S. Connors, R. J. Bendura, J. L. Raper, G. W. Sachse, J. C. Gille, L. Emmons, and C. L. Heald (2003), The Transport and Chemical Evolution over the Pacific (TRACE-P) aircraft mission: Design, execution, and first results, *J. Geophys. Res.*, *108*(D20), 9000, doi:10.1029/2002JD003276.

Jaecker-Voirol, A., and P. Mirabel (1989), Heteromolecular nucleation in the sulfuric acid-water system, *Atmos. Environ.*, *23*, 2053–2057.

Janson, R., K. Rosman, A. Karlsson, and H.-C. Hansson (2001), Biogenic emissions and gaseous precursors to forest aerosols, *Tellus, Ser. B*, *53*, 423–440.

Jordan, C. E., J. Dibb, B. E. Anderson, and H. E. Fuelberg (2003), Uptake of nitrate and sulfate on dust aerosols during TRACE-P, *J. Geophys. Res.*, *108*(D21), 8817, doi:10.1029/2002JD003101.

Kerminen, V.-M., and A. S. Wexler (1994a), Particle formation due to SO_2 oxidation and high relative humidity in the remote marine boundary layer, *J. Geophys. Res.*, *99*(D12), 25,607–25,614.

Kerminen, V.-M., and A. S. Wexler (1994b), Post-fog nucleation of H_2SO_4-H_2O particles in smog, *Atmos. Environ.*, *28*, 2399–2406.

Kulmala, M., A. Laaksonen, and L. Pirjola (1998), Parameterizations for sulfuric acid/water nucleation rates, *J. Geophys. Res.*, *103*(D7), 8301–8308.

Kulmala, M., M. Dal Maso, J. M. Makela, L. Pirjola, M. Vakeva, P. Aalto, P. Miikkulainen, K. Hameri, and C. D. O'Dowd (2001a), On the formation, growth and composition of nucleation mode particles, *Tellus, Ser. B*, *53*, 479–490.

Kulmala, M., et al. (2001b), Overview of the international project on biogenic aerosol formation in the boreal forest, *Tellus, Ser. B*, *53*, 324–343.

Kulmala, M., P. Korhonen, I. Napari, A. Karlsson, H. Berresheim, and C. D. O'Dowd (2002), Aerosol formation during PARFORCE: Ternary nucleation of H_2SO_4, NH_3, and H_2O, *J. Geophys. Res.*, *107*(D19), 8111, doi:10.1029/2001JD000900.

Kulmala, M., H. Vehkamäki, T. Petäjä, M. Dal Maso, A. Lauri, V.-M. Kerminen, W. Birmili, and P. H. McMurry (2004), Formation and growth rates ofultrafine atmospheric particles: a review of observations, *J. Aerosol Sci.*, *35*(2), 143–176.

Leaitch, W. R., J. W. Bottenheim, T. A. Biesenthal, S.-M. Li, P. S. K. Liu, K. Asalian, H. Dryfhout-Clark, F. Hopper, and F. Brechtel (1999), A case study of gas-to-particle conversion in an eastern Canadian forest, *J. Geophys. Res.*, *104*(D7), 8095–8111.

Liu, H., D. J. Jacob, I. Bey, R. M. Yantosca, B. N. Duncan, and G. W. Sachse (2003), Transport pathways for Asian combustion outflow over the Pacific: Interannual and seasonal variability, *J. Geophys. Res.*, *108*(D1), 4006, doi:10.1029/2001JD001395.

Marti, J. J., R. J. Weber, M. T. Saros, J. G. Vasiliou, and P. H. McMurry (1996), Modification of the TSI 3025 condensation particle counter for pulse height analysis, *Aerosol Sci. Technol.*, *25*, 214–218.

Moore, K. G. I., A. D. Clarke, C. N. Kapustin, and S. Howell (2003), Long-range transport of continental plumes over the Pacific Basin: Aerosol physiochemistry and optical properties during PEM-Tropics A and B, *J. Geophys. Res.*, *108*(D2), 8236, doi:10.1029/2001JD001451.

Napari, I., M. Kulmala, and H. Vehkamäki (2002a), Ternary nucleation of inorganic acids, ammonia and water, *J. Chem. Phys.*, *117*(18), 8418–8425, doi:10.1063/1.151722.

Napari, I., M. Noppel, H. Vehkamäki, and M. Kulmala (2002b), An improved model for ternary nucleation of sulfuric acid-ammonia-water, *J. Chem. Phys.*, *116*(10), 4221–4227, doi:10.1063/1.1450557.

Napari, I., M. Noppel, H. Vehkamäki, and M. Kulmala (2002c), Parameterization of ternary nucleation rates for H_2SO4-NH_3-H_2O vapors, *J. Geophys. Res.*, *107*(D19), 4381, doi:10.1029/2002JD002132.

Nilsson, E. D., and M. Kulmala (1998), The potential for atmospheric mixing to enhance the binary nucleation rate, *J. Geophys. Res.*, *103*(D1), 1381–1389.

Nilsson, E. D., J. Paatero, and M. Boy (2001), Effects of air masses and synoptic weather on aerosol formation in the continental boundary layer, *Tellus, Ser. B*, *53*, 462–478.

O'Dowd, C. D., et al. (2002a), Coastal new particle formation: Environmental conditions and aerosol physicochemical characteristics during

nucleation bursts, *J. Geophys. Res.*, *107*(D19), 8107, doi:10.1029/2000JD000206.

O'Dowd, C. D., et al. (2002b), A dedicated study of New Particle Formation and Fate in the Coastal Environment (PARFORCE): Overview of objectives and achievements, *J. Geophys. Res.*, *107*(D19), 8108, doi:10.1029/2001JD000555.

Orsini, D., Y. Ma, A. Sullivan, B. Sierau, K. Baumann, and R. J. Weber (2003), Refinements to the particle-into-liquid sampler (PILS) for ground and airborne measurements of water soluble aerosol composition, *Atmos. Environ.*, *37*, 1243–1259.

Pirjola, L., C. D. O'Dowd, I. M. Brooks, and M. Kulmala (2000), Can new particle formation occur in the clean marine boundary layer?, *J. Geophys. Res.*, *105*(D21), 26,531–26,546.

Raes, F., R. V. Dingenen, E. Vignati, J. Wilson, J. P. Putaud, J. H. Seinfeld, and P. Adams (2000), Formation and cycling of aerosols in the global troposphere, *Atmos. Environ.*, *34*, 4215–4240.

Russell, L. M., R. Caldow, M. R. Stolzenburg, S.-H. Zhang, R. C. Flagan, and J. H. Seinfeld (1996), Radially-classified aerosol discriminator for aircraft-based time-resolved ultrafine size-distribution measurements, *J. Atmos. Oceanic Technol.*, *13*, 598–609.

Saros, M. T., R. J. Weber, J. J. Marti, and P. H. McMurry (1996), Ultrafine aerosol measurement using a condensation nucleus counter with pulse height analysis, *Aerosol Sci. Technol.*, *25*, 200–213.

Seinfeld, J. H., and S. N. Pandis (1998), *Atmospheric Chemistry and Physics*, John Wiley, New York.

Stratmann, F., et al. (2003), New-particle formation events in a continental boundary layer: First results from the SATURN experiment, *Atmos. Chem. Phys.*, *3*, 1445–1459.

Streets, D. G., et al. (2003), An inventory of gaseous and primary aerosol emissions in Asia in the year 2000, *J. Geophys. Res.*, *108*(D21), 8809, doi:10.1029/2002JD003093.

Tang, Y., et al. (2004), Three-dimensional simulations of inorganic aerosol distributions in east Asia during spring 2001, *J. Geophys. Res.*, *109*, D19S23, doi:10.1029/2003JD004201, in press.

Thornton, D. C., A. R. Bandy, F. H. Tu, B. W. Blomquist, G. M. Mitchell, W. Nadler, and D. H. Lenschow (2002), Fast airborne sulfur dioxide measurements by Atmospheric Pressure Ionization Mass Spectrometry (APIMS), *J. Geophys. Res.*, *107*(D22), 4632, doi:10.1029/2002JD002289.

Twomey, S. (1974), Pollution and the planetary albedo, *Atmos. Environ.*, *8*, 1251–1256.

Vehkamäki, H., M. Kulmala, I. Napari, K. E. J. Lehtinen, C. Timmreck, M. Noppel, and A. Laaksonen (2002), An improved parameterization for sulfuric acid-water nucleation rates for tropospheric and stratospheric conditions, *J. Geophys. Res.*, *107*(D22), 4622, doi:10.1029/2002JD002184.

Verheggen, B., and M. Mozurkewich (2002), Determination of nucleation and growth rates from observation of a SO_2 induced atmospheric nucleation event, *J. Geophys. Res.*, *107*(D11), 4123, doi:10.1029/2001JD000683.

Weber, R. J., J. J. Marti, P. H. McMurry, F. L. Eisele, D. J. Tanner, and A. Jefferson (1997), Measurements of new particle formation and ultrafine particle growth rates at a clean continental site, *J. Geophys. Res.*, *102*(D4), 4375–4385.

Weber, R. J., P. H. McMurry, R. L. Mauldin, D. J. Tanner, F. L. Eisele, F. J. Brechtel, S. M. Kreidenweis, G. L. Kok, R. D. Schillawski, and D. Baumgardner (1998a), A study of new particle formation and growth involving biogenic and trace gas species measured during ACE-1, *J. Geophys. Res.*, *103*(D13), 16,385–16,396.

Weber, R. J., M. Stolsenburg, S. Pandis, and P. H. McMurry (1998b), Inversion of the UCNC pulse height distributions to obtain ultrafine (~3–10 nm) particle size distributions, *J. Aerosol Sci.*, *29*, 601–615.

Weber, R. J., G. Chen, D. D. Davis, R. L. Mauldin, D. J. Tanner, F. L. Eisele, A. D. Clarke, D. C. Thornton, and A. R. Bandy (2001a), Measurements of enhanced H_2SO_4 and 3–4 nm particles near a frontal cloud during the First Aerosol Characterization Experiment (ACE-1), *J. Geophys. Res.*, *106*(D20), 24,107–24,117.

Weber, R. J., D. Orsini, Y. Duan, Y. N. Lee, P. J. Klotz, and F. Brechtel (2001b), A particle-into-liquid collector for rapid measurements of aerosol bulk chemical composition, *Aerosol Sci. Technol.*, *35*, 718–727.

Weber, R. J., et al. (2003), New particle formation in anthropogenic plumes advecting from Asia observed during TRACE-P, *J. Geophys. Res.*, *108*(D21), 8814, doi:10.1029/2002JD003112.

Wexler, A. S., L. F. W., and J. H. Seinfeld (1994), Modeling urban and regional aerosols: 1. Model development, *Atmos. Environ.*, *28*, 531–546.

Wilemski, G. (1984), Composition of the critical nucleus in multicomponent vapor nucleation, *J. Chem. Phys.*, *80*(3), 1370–1372.

A. R. Bandy and D. C. Thornton, Department of Chemistry, Drexel University, 32nd and Chestnut Streets, Philadelphia, PA 19104, USA. (bandyar@drexel.edu; thorntdc@drexel.edu)

B. Blomquist, V. Brekhovskikh, A. D. Clarke, S. G. Howell, C. S. M^{c}Naughton, and K. G. Moore II, School of Ocean and Earth Science and Technology, University of Hawaii, 1000 Pope Road, Honolulu, HI 96822, USA. (blomquis@hawaii.edu; verab@soest.hawaii.edu; tclarke@soest.hawaii.edu; showell@soest.hawaii.edu; cameronm@soest.hawaii.edu; kmoore@soest.hawaii.edu)

F. J. Brechtel, Brechtel Manufacturing Inc., 1789 Addison Way, Hayward, CA 94544-6900, USA. (fredb@bnl.gov)

G. Buzorius, CIRPAS, Naval Postgraduate School, 3200 Imjin Road, Hangar 507, Marina, CA 93933, USA. (gintas@nps.edu)

G. R. Carmichael and Y. Tang, Department of Chemical and Biochemical Engineering, University of Iowa, Iowa City, IA 52242-1000, USA. (gcarmich@icaen.uiowa.edu; ytang@cgrer.uiowa.edu)

D. S. Covert, Department of Atmospheric Sciences, University of Washington, Box 354235, Seattle, WA 98195, USA. (dcovert@u.washington. edu)

F. L. Eisele and R. L. Mauldin, Atmospheric Chemistry Division, National Center for Atmospheric Research, 1850 Table Mesa Drive, Boulder, CO 80303, USA. (eisele@ucar.edu; mauldin@ucar.edu)

D. A. Orsini and R. J. Weber, School of Earth and Atmospheric Sciences, Georgia Institute of Technology, 221 Boddy Dodd Way, Atlanta, GA 30332, USA. (douglas.orsini@eas.gatech.edu; rweber@eas.gatech.edu)